



Proteasome $\alpha 6$ Subunit Negatively Regulates the JAK/STAT Pathway and Blood Cell Activation in *Drosophila melanogaster*

Mirva Järvelä-Stölting^{1†}, Laura Vesala^{1†}, Matthew K. Maasdorp¹, Joanna Ciantar¹, Mika Rämetsä^{1,2,3,4} and Susanna Valanne^{1*}

¹ Laboratory of Experimental Immunology, Faculty of Medicine and Health Technology, Tampere University, Tampere, Finland, ² Research Unit for Pediatrics, Pediatric Neurology, Pediatric Surgery, Child Psychiatry, Dermatology, Clinical Genetics, Obstetrics and Gynecology, Otorhinolaryngology and Ophthalmology, Faculty of Medicine, University of Oulu, Oulu, Finland, ³ Medical Research Center Oulu, University of Oulu, Oulu, Finland, ⁴ Department of Children and Adolescents, Oulu University Hospital, University of Oulu, Oulu, Finland

OPEN ACCESS

Edited by:

Shoichiro Kurata,
Tohoku University, Japan

Reviewed by:

Marie-Odile Fauvarque,
CEA Grenoble, France
Michele Crozatier,
UMR5547 Centre de Biologie du
Développement (CBD), France

*Correspondence:

Susanna Valanne
susanna.valanne@tuni.fi

[†]These authors have contributed
equally to this work

Specialty section:

This article was submitted to
Comparative Immunology,
a section of the journal
Frontiers in Immunology

Received: 23 June 2021

Accepted: 30 November 2021

Published: 22 December 2021

Citation:

Järvelä-Stölting M, Vesala L,
Maasdorp MK, Ciantar J, Rämetsä M
and Valanne S (2021) Proteasome $\alpha 6$
Subunit Negatively Regulates the JAK/
STAT Pathway and Blood Cell
Activation in *Drosophila melanogaster*.
Front. Immunol. 12:729631.
doi: 10.3389/fimmu.2021.729631

JAK/STAT signaling regulates central biological functions such as development, cell differentiation and immune responses. In *Drosophila*, misregulated JAK/STAT signaling in blood cells (hemocytes) induces their aberrant activation. Using mass spectrometry to analyze proteins associated with a negative regulator of the JAK/STAT pathway, and by performing a genome-wide RNAi screen, we identified several components of the proteasome complex as negative regulators of JAK/STAT signaling in *Drosophila*. A selected proteasome component, *Pros $\alpha 6$* , was studied further. In S2 cells, *Pros $\alpha 6$* silencing decreased the amount of the known negative regulator of the pathway, ET, leading to enhanced expression of a JAK/STAT pathway reporter gene. Silencing of *Pros $\alpha 6$* *in vivo* resulted in activation of the JAK/STAT pathway, leading to the formation of lamellocytes, a specific hemocyte type indicative of hemocyte activation. This hemocyte phenotype could be partially rescued by simultaneous knockdown of either the *Drosophila* STAT transcription factor, or MAPKK in the JNK-pathway. Our results suggest a role for the proteasome complex components in the JAK/STAT pathway in *Drosophila* blood cells both *in vitro* and *in vivo*.

Keywords: *Drosophila melanogaster*, fruit fly, JAK/STAT pathway, Eye Transformer, the proteasome complex, hemocyte, lamellocyte, RNA interference

INTRODUCTION

Regulation of blood cell differentiation and function is a central aspect in immune responses in animals. In addition to the effective activation of the immune cells, controlled silencing of activation is equally important; constant immune cell activity consumes energy and leads to detrimental processes such as autoimmune reactions (1, 2). The Janus kinase/signal transducers and activators

Abbreviations: AMPs, Antimicrobial peptides; dsRNA, double-stranded RNA; GFP, Green Fluorescent Protein; hop^{Tum-1}, Hopscotch Tumorous-lethal; He, hemese; hep, hemipterous; Hml, Hemolectin; imd, Immune Deficiency; JAK, Janus kinase; JNK, c-Jun terminal kinase; STAT, Signal Transducer Activator of Transcription; pMT, plasmid with a metallothionein promoter; RNAi, RNA interference; TotM, Turandot M; UAS, Upstream Activating Sequence; upd, Unpaired.

of transcription (JAK/STAT) signaling is involved in controlling and regulating biological functions including cell differentiation, developmental processes and immune responses (3). In humans, JAK/STAT is central for blood cell homeostasis, and its aberrant activation can lead to myeloproliferative neoplasms (4, 5). In *Drosophila*, misregulated JAK/STAT signaling in blood cells leads to blood cell activation and formation of tumor-like melanotic blood cell clusters (6–8). The *Drosophila* larval blood cell system consists of three main types of hemocytes: plasmatocytes, lamellocytes and crystal cells (9, 10). Plasmatocytes, the main blood cell type, are round, macrophage-like cells found in all developmental stages in the circulation and in reservoir compartments (11–13). Plasmatocytes are responsible for the phagocytosis of pathogens and apoptotic cells (12, 14, 15). Lamellocytes are a specialized hemocyte type, produced as a response to infection by parasitoid wasps and other pathogens that cannot be phagocytosed (16). They encapsulate the intruder and produce melanin to seal the capsule (17). The third group is crystal cells, which function in the melanization response that is essential for wound healing (18, 19). The activation of several signaling pathways, including the JAK/STAT, Toll, Ras-MAPK and the c-Jun N-terminal kinase (JNK) signaling pathways, is known to induce lamellocyte formation (6, 20).

Drosophila JAK/STAT signaling is simpler than its human counterpart, and therefore *Drosophila* offers a prominent model for studying the JAK/STAT pathway, particularly *in vivo* (21). Instead of tens of ligands, four JAKs and seven STATs in humans (22), *Drosophila* only has one JAK (Hopscotch), one STAT (STAT92E) (23, 24) and three cytokine-like ligands (Upd1, Upd2 and Upd3) (25, 26). The signaling pathway is activated when one of the three ligands binds to the receptor Domeless (Dome), a *Drosophila* homolog to the human GP130 receptor (27). Ligand binding leads to the dimerization of Dome and thus, activation of the tyrosine kinase Hopscotch (Hop) (28). Hop activation induces the phosphorylation of the intracellular part of Dome, transphosphorylation of Hop and enables the SH2 domain of the STAT92E transcription factor to attach to the receptor. Hence, Hop phosphorylates STAT92E which dimerizes and translocates to the nucleus where it activates the target genes of the JAK/STAT pathway (29). Similarly to its mammalian counterpart, the *Drosophila* JAK/STAT pathway is involved in several processes including development, stem cell maintenance, immune and stress responses and larval hematopoiesis (25, 30).

Due to its key role in regulating blood cells both in mammals and in insects, it is important to understand the negative and positive regulatory events controlling the activity of the JAK/STAT pathway. We aimed at identifying novel factors that would interact with a known negative regulator of *Drosophila* JAK/STAT signaling, the Eye transformer (ET/CG14225) (31, 32), and therefore participate in the regulation of JAK/STAT activity. In our mass spectrometry study in S2 cells harboring a hemocyte-like identity, we identified several members of the proteasome complex as interactors of ET. Furthermore, we show that silencing *Proteasome α6 subunit in vivo* in *Drosophila* hemocytes induces JAK/STAT activation in them, leading to

typical JAK/STAT induced hemocyte phenotypes, the appearance of melanotic nodules and the formation of different types of hemocytes usually present after an immune challenge. Hence, we show that proper functioning of the proteasome complex is crucial for keeping JAK/STAT signaling at bay in hemocytes in healthy animals.

MATERIALS AND METHODS

dsRNA Synthesis

dsRNAs were produced as described previously (31). The primers used for dsRNA synthesis are listed in **Supplementary Table 1**.

Cell Culture, Transient Transfections and Reporter Assays

The *Drosophila* S2 cells were cultured at 25°C in Schneider's Insect medium (Sigma, Cat#S9895-1L, USA) containing 0.4 g NaHCO₃ (Sigma Cat#22350-6, USA) and 0.8 g CaCl₂ · 2 H₂O (Sigma S5791-500g, Germany), 10% heat-inactivated Fetal Bovine Serum, FBS (Sigma, Cat#F7524, France) and 50 U/ml Penicillin/Streptomycin (Biochrom AG, Cat#A2213, Berlin).

The S2 cells were transiently transfected using Fugene6 reagent (Roche, Basel, Switzerland) following the manufacturer's instructions. The JAK/STAT pathway was activated by transfection with either the constitutively active pMT-*hop^{Tum-1}* or with the pMT-*upd1-myc* plasmid. To measure the JAK/STAT pathway activation, a *Turandot M-luciferase* (*TotM-luc*) reporter construct, a kind gift from Professor Jean-Luc Imler (University of Strasbourg, France), was used. For studying the effect of RNAi knockdown of selected genes on the expression of ET-V5, S2 cells were transfected with either the pMT-empty or pMT-*Upd1* plasmids together with the pMT-*ET-V5* plasmid and selected dsRNAs. For studying the effect of RNAi knockdown of selected genes on the expression of endogenous *STAT92E*, S2 cells were transfected with the pMT-*Upd1* plasmid for induction of the JAK/STAT pathway. The pMT-empty plasmid was used as a control for uninduced conditions. The protein production from the pMT plasmids was induced 24–48h post transfection by adding CuSO₄ to each well to a final concentration of 250–500 μM. For Toll and Imd pathway reporter assays, a *Spätzle* or *Imd* overexpressing plasmid was used to induce the pathway and *Drosomycin-luc* or *Attacin-luc* was used as the reporter, respectively (33, 34). In all reporter assays, an Actin5C-β-galactosidase reporter plasmid was used to normalize the results for transfection efficiency and cell numbers as described previously (31). Luciferase and β-galactosidase reporter assays were carried out as previously described in (31).

Stable Transfection of S2 Cells With Selected Plasmids

The S2 cells were stably transfected with 9.5 μg of each plasmid construct (empty pMT-vector or pMT-*ET-V5* ± pMT-*upd1-myc*) together with 0.5 μg of the coHygro plasmid to enable Hygromycin-B selection of transfected cells. Transfections were carried out on 6-well plates using the Fugene6 transfection

reagent (Roche, Basel, Switzerland). Three days post-transfection the transfected cells were selected by adding medium containing 150–300 µg/ml of Hygromycin-B (HyClone Laboratories, Inc. USA). The Hygromycin-B concentration was increased in every passaging up to 300 µg/ml. Under Hygromycin-B selection, only cells carrying the coHygro plasmid survive. From here onwards, the cells were grown under Hygromycin selection.

Cell Lysis, Protein Extraction and Protein Concentration Measurement

24–48h after the protein production from the pMT-plasmids was induced with CuSO₄, the cells from three pooled wells, each containing 3 ml of S2 cell suspension, were collected per sample and centrifuged at 5000 x g for 3 min. The supernatants were discarded and 900 µl of lysis buffer (1 x PBS, 1% Igepal CA-630 [Sigma-Aldrich/Merck, Darmstadt, Germany], 0.5% Sodium deoxycholate, 0.1% SDS, 2 mM EDTA, Halt™ Protease and Phosphatase Inhibitor Cocktail, EDTA-free [Thermo Fisher Scientific Inc.]) was added to each sample. The samples were left to lyse on ice for 30 min. The lysates were centrifuged at 16 000 x g for 10 min and the cleared lysates were transferred into new tubes. The protein concentration of each lysate was measured with the Pierce™ BCA protein Assay Kit (Pierce®, #23227, USA) according to the manufacturer's instructions.

Co-Immunoprecipitation of Protein Complexes With the V5 Antibody, SDS-PAGE and Silver Staining

Putative ET-interaction partners were co-immunoprecipitated from S2 cell protein lysates using Anti-V5 Agarose Affinity Gel (Sigma, #A7345, Israel) according to the manufacturer's instructions. The following lysates were used: S2 cells (neg. ctrl 1), empty pMT-vector (neg. ctrl 2), pMT-ET-V5 and pMT-ET-V5 + pMT-*upd1-myc*. 900 µl of each lysate, containing approximately 2.5 mg of protein, was incubated overnight with the Anti-V5 Agarose Affinity Gel, after which the complexes were washed 6 x 10 minutes with PBS containing protease and phosphatase inhibitor cocktail. All incubations and treatments were carried out at 4°C or on ice. Finally, loading buffer was added on the washed affinity gel containing protein complexes and the samples were boiled to release the proteins. Purified protein complexes were analyzed by SDS-PAGE and silver-staining.

For SDS-PAGE, Novex 10% NuPAGE Bis-Tris (Life Technologies, #NP0301BOX, USA) gels were used. Precision Plus Protein™ Dual Xtra Standard (Bio-Rad, #161-0377, USA) was used as a marker. The electrophoresis was carried out for 45 min using MOPS buffer and NuPAGE Gel program (200 V, 120 mA, 25 W). To stain the protein bands on the gel, the Pierce® Silver Stain for Mass Spectrometry kit (Thermo Scientific, #24600, USA) was used according to the manufacturer's instructions.

Mass Spectrometry and Identification of Protein Complex Components

The anti-V5 antibody purified samples were analyzed by mass spectrometry with the help of Tuula Nyman at the University of

Helsinki. To identify the proteins in complex with ET, the anti-V5 purified lysates were separated on SDS-PAGE gels and silver stained as described above. The whole sample lanes on SDS-PAGE gel were cut into equal sized pieces after which an in-gel trypsin digestion was performed. The digested peptides were analyzed as described in (35). Flybase Query and Blast tools were used to process the obtained data. The data from the LC-MS/MS was searched against the SwissProt database through ProteinPilot with MASCOT. The following MASCOT search parameters were used: *Drosophila melanogaster* as species, carbamidomethyl modification of cysteine as a fixed modification and oxidation of methionine as a variable modification, trypsin digestion allowing one missed cleavage, 50 ppm mass tolerance and 0.2 Da fragment tolerance for peptides. False discovery rates for the LC-MS/MS data were 1.5–4%.

SDS-PAGE, Western Blotting and Protein Band Intensity Analysis

For studying the effect of RNAi knockdown of selected genes on the expression of pMT-ET-V5, protein lysates were prepared as above and the production of the ET-V5 protein was analyzed by SDS-PAGE and Western blotting. The total protein content of the lysates was set to 50 µg/lane. For SDS-PAGE, Biorad TGX 4–20% mini gels (Bio-Rad, #456-1093, USA) were used. PageRuler™ Prestained protein ladder (Thermo Scientific #26616, Lithuania) was used as a marker. The electrophoretic separation of proteins was carried out for 20–25 min with 300 V using the Tris/Glycine/SDS buffer (Bio-Rad #1610732, USA).

For Western blotting, proteins were transferred from the SDS-PAGE gel either onto 0.45 µm nitrocellulose membrane (Hybond-C extra; Amersham Biosciences, RPN203E, United Kingdom) using the wet transfer technique with an in-house transfer buffer (25 mM Tris, 192 mM glycine, 8% methanol) and the NuPAGE Blot program (25 V, 160 mA, 1 h 15 min), or onto 0.2 µm nitrocellulose membrane using Trans-Blot turbo transfer packs (Bio-Rad, #1704158, USA) and equipment according to the manufacturer's instructions for TGX mini-gels. The membranes containing the transferred proteins were first incubated with blocking buffer (5% skimmed milk powder in PBS + 0.05% Tween 20 [PBST]) for 2 h at RT or overnight at 4°C. After blocking, the membranes were incubated with primary antibodies in blocking buffer for either 1–2h at RT or overnight at 4°C. The following antibodies were used: anti-V5-HRP conjugate (1:3000, Invitrogen™, Life Technologies, P/N 46-0708), anti-V5 antibody (1:3000, Invitrogen™, Life Technologies P/N 46-0705) and α-tubulin antibody (1:1000, clone DM1A, Sigma-Aldrich). After incubation, the membranes were rinsed three times with PBST and further washed with PBST 4 x 5 min at RT. Goat anti-mouse IgG (H+L) HRP secondary antibody (1:5000, ThermoFisher #G-21040) was used for detecting the mouse monoclonal antibodies (V5 antibody, α-tubulin antibody). Secondary antibody was incubated for 1 h at RT, after which the membranes were washed as before. Immunostained proteins were visualized using an ECL Western Blotting Detection Reagent (either with #RPN2232 by GE Healthcare Amersham™, UK or Westernbright,

Advansta, USA) and imaged with the BioRad ChemiDoc™ MP imager using the BioRad ImageLab software (Bio-Rad, California, USA) or by developing the signal on an X-ray film (Fuji Super RX-N film, Japan).

To estimate the amounts of the proteins of interest produced, band intensities on exposed films or imager images were analyzed with the Fiji-ImageJ-64-bit (ver1.51) software. Briefly, images were saved in grayscale in 32-bit mode, after which the bands to be analyzed were selected and their intensities plotted. The intensity of the ET-V5 protein band from the cell lysate was normalized to α -tubulin signal from that lysate. Plotted values were normalized to the control (GFP dsRNA-treated) protein band value. Per phenotype, 6-7 replicates were analyzed.

Fly Stocks

We utilized the GAL4/UAS system (36) to target the expression of transgenes into the fly blood cells, the hemocytes. To visualize larval hemocytes we used the *eaterGFP* (37) and *msnCherry* (38) fluorescent reporters for plasmatocytes and lamellocytes, respectively. These reporters were combined with two hemocyte drivers, *P{Hml-GAL4.Δ}2* [Bloomington *Drosophila* Stock Center, BL #30139 (39)], and *P{He-GAL4.Z}85* [BL #8699 (6)], in order to simultaneously visualize hemocytes and to express transgenic constructs in them, resulting in fly strain *yw,msnF9mo-mCherry, eaterGFP;Hml^Δ-GAL4;He-GAL4*, hereafter called *mCherry, eaterGFP;Hml^Δ-GAL4;He-GAL4*. For suppression of gene expression by RNA interference (RNAi), we used the following transgenic lines obtained from the Vienna *Drosophila* Resource Center (VDRC) GD (P-element) and KK (phiC31) RNAi stocks: *UAS-Proα6^{GD}* (VDRC ID #26653), *UAS-Proα6^{KK}* (#100703), *UAS-Stat92E^{GD}* (#43867) and *UAS-hep^{GD}* (#2968). The VDRC *w¹¹¹⁸* strains #60100 (denoted as *w^{KK}*) and #60000 (denoted as *w^{GD}*) were used as genetic background controls for the KK and GD stocks, respectively. The following combination lines were generated: *w; UAS-Proα6^{GD}* (#26653); *UAS-Stat92E^{GD}* (#43867) and *UAS-hep^{GD}* (#2968); *UAS-Proα6^{GD}* (#26653); +. For testing the *UAS-Proα6-RNAi* silencing efficiencies, we used a combination of the hemocyte drivers mentioned above, that also contain two inserts of *UAS-eGFP* (*w; HmlΔ -GAL4, UAS-eGFP; He-GAL4, UAS-eGFP*). Of note, to denote the presence of the GAL4/UAS in the figures, we use the symbol “>”.

For detecting the JAK/STAT activity *in vivo*, the *10xStat92E-GFP* [BL #26197 (40)], reporter combined with *He-GAL4* to get *10xSTAT92E-GFP; He-GAL4* was used (a gift from Prof. Dan Hultmark). To activate JAK/STAT signaling, the constitutively active form of *Drosophila* JAK, *UAS-hop^{Tum-1}* (41) was expressed in hemocytes. 15-20 females of a driver or genetic background control line were crossed with 10 males from transgenic construct lines and kept at 25°C and 12:12 light:dark cycle (LD12:12). Flies were placed daily in fresh vials, and vials with eggs were transferred to 29°C and LD12:12.

Flow Cytometry Analysis of Larval Hemocytes

Late 3rd instar larvae were washed in water with a brush until clean, placed in a 20 μ l drop of 8% bovine serum albumin (BSA)

in 1 x phosphate buffered saline (PBS) and carefully ripped open using forceps. The hemolymph was allowed to bleed out and the carcass was removed. The hemolymph sample was pipetted into a 1.5 ml Eppendorf tube with 80 μ l of 8% BSA in PBS. 30 μ l of the sample was run with a BD Accuri C6 flow cytometer (Becton, Dickinson & Company). Each genotype was analyzed in triplicate (3 x 10 larvae). For the *eaterGFP* and *msnCherry* reporter analysis, a 488 nm 50 mW solid-state laser and 510 +/- 15 nm (FL1, GFP) and 610 +/- 20 nm (FL3, mCherry) optical filters were used to capture the fluorescence signal. GFP-only, mCherry-only and non-fluorescent hemocytes were used to check for the location of these hemocytes and to deduct fluorescence spill over into a wrong channel. By using these reporters, five hemocyte populations can be detected, consisting of single and double positive hemocytes. Following the naming strategy presented in (42), these hemocyte are: plasmatocytes (GFP^{high}), activated plasmatocytes (GFP^{high},mCherry^{low}), lamelloblasts (GFP^{low}), prelamellocytes (GFP^{low},mCherry^{low}) and mature lamellocytes (mCherry^{high}). The complete procedure of the hemocyte flow cytometry with gating strategies is described in (42).

For the *10xStat92E-GFP* reporter fluorescence measurement, the hemocyte population was separated from the debris based on forward scatter (FSC-A) and side scatter (SSC-A). This population was gated and used in subsequent analyses. A 488 nm 50 mW solid-state laser was used to excite the green fluorescent protein (GFP) and the emission was detected using a 510 +/- 15 nm (FL1) optical filter. Non-fluorescent hemocytes (*w^{GD}*) were used as a negative control and hemocytes with *hop^{Tum-1}* overexpression (*10xStat92E-GFP;He-GAL4/UAS-hop^{Tum-1}*) as a positive control. Hemocytes with a fluorescence intensity above the autofluorescence of the hemocytes in the FL1 channel were considered GFP-positive. A forward scatter area vs. height plot (FSC-A vs. FSC-H) was used to define the population of round hemocytes, representing the majority of hemocytes in a healthy *Drosophila* larva, the plasmatocytes. These hemocytes were gated, and the GFP fluorescence intensity was measured for all hemocytes gated in the FSC-SSC plot and separately only for the hemocytes falling into the plasmatocyte gate.

Hemocyte Imaging

3rd instar larvae were bled in a drop of 1% BSA in PBS on a 12-well glass slide, pooling hemocytes from three larvae per well. Hemocytes were allowed to attach and spread on the slide for 50 min, after which they were fixed for ten minutes using 20 μ l of 3.7% paraformaldehyde. After fixation, wells were washed three times using cold 1 x PBS and permeabilized for 5 min using 0.1% Triton-X100. After washing three times using cold 1 x PBS, cells were incubated for 30 min with 20 μ l of Alexa Fluor 680 -conjugated Phalloidin (Invitrogen), in a 1:50 dilution in 1% BSA in PBS, to stain filamentous actin. The wells were washed, and the samples mounted using ProLong Gold antifade reagent with DAPI (ThermoFisher Scientific) and Zeiss coverslips (thickness no. 1 ½, 18 x 18 mm). Slides were left to cure overnight at room temperature protected from light and imaged with Zeiss LSM 780 laser scanning confocal microscope using a 40x oil immersion objective at several

random locations on the next day. 405 nm, 488 nm and 628 nm lasers were used to excite DAPI, GFP and AlexaFluor 688 nm, respectively, and emission was collected at 410-488 nm, 490-544 nm and 661-759 nm. Multiple layers were imaged in Z-plane at 0.36 μm intervals. ImageJ version 2.1.0/1.53 c was utilized to create stacked images. ImageJ and Adobe Photoshop (release 22.5.1) were used to enhance the fluorescence signal for better visibility, keeping modifications constant across the images.

Pupation and Ecdysis Success and Larval and Pupal Melanotic Nodules

The effect of silencing *Prosα6* in hemocytes on the number of successfully pupated and eclosed animals was assessed in *msnCherry, eaterGFP; Hml^A-GAL4; He-GAL4* flies crossed with *UAS-Prosα6^{GD}*, *UAS-Prosα6^{KK}* and *w^{GD}* flies. Three to four replicate crosses of each genotype were made, and adults were transferred to fresh vials on three subsequent days. Eggs were counted from each vial and the vials were monitored daily for pupated/eclosed animals. At the same time, the number of pupae with melanotic nodules was recorded. Examples of pupae with melanotic nodules were imaged with a Nikon DS-Fi2 camera attached to a Nikon SMZ745T microscope and a Nikon DS-L3 camera control unit.

The prevalence of larval melanotic nodules was assessed for the same genotypes in three replicate crosses (100 animals each) by inspecting the larvae under a stereomicroscope. Example images of larvae (20x magnification) were taken with a Deltapix Invenio 10EIII camera (DeltaPix, Denmark) attached to a Nikon SMZ745T stereomicroscope using the DeltaPix InSight software.

Lifespan Experiment

The effect of silencing *Prosα6* in hemocytes on the viability of the flies was assessed by monitoring the lifespan of the flies compared to controls. *UAS-Prosα6^{GD}* and *UAS-Prosα6^{KK}* RNAi lines were crossed with the *msnCherry, eaterGFP; Hml^A-GAL4; He-GAL4* flies (described above) at 25°C. As a control, *msnCherry, eaterGFP; Hml^A-GAL4; He-GAL4* flies were crossed with *w^{GD}* flies. The fly eggs were transferred to 29°C, and this temperature was used for the entire lifespan of the flies. Every 2-3 days the number of living flies was recorded, and the flies were transferred to fresh food.

RNA Extraction and qRT-PCR from S2 Cells and Hemocytes

Expression levels of selected genes in S2 cells and hemocytes were measured by quantitative reverse transcriptase PCR (qRT-PCR) from extracted RNA. For monitoring expression levels in S2 cells, the cells were grown on 24-well plates, treated with selected dsRNAs and transfected with selected plasmids as described above. For studying expression levels in hemocytes *in vivo*, hemocytes from 50 dissected larvae were collected for each replicate; three biological replicates from three independent crosses were used per genotype. The RNA extraction both from hemocytes and cultured cells was performed using the TRI reagent (MRC, Thermo Fisher Scientific). S2 cells were harvested from culture

plates by pipetting and centrifugation (5000 x g, 3 min), after which cells were homogenized and lysed in TRI reagent by pipetting up and down at least 10 times. Extraction from hemocytes was started by adding TRI reagent onto the frozen hemocyte pellet, and cells were homogenized and lysed by pipetting up and down at least 10 times. Thereafter the extraction was performed according to manufacturer's instructions. qRT-PCR was carried out from extracted RNAs (30-40 ng RNA/sample) using the iTaq Universal SYBR Green OneStep kit (Bio-Rad, Hercules, CA). The expression values obtained for selected genes were normalized to the expression of a gene encoding for ribosomal protein L32 (*RpL32*). The primers used are listed in **Supplementary Table 1**.

Statistics

Statistical analyses of luciferase assay measurements, qRT-PCR results and protein band intensity analyses were carried out using the two-tailed Student t-test for two arrays assuming equal variances. Statistical analyses of fly life span experiments were carried out with the log-rank (Mantel-Cox) test using Prism 6 (GraphPad) software. The difference was considered statistically significant if the p-value was < 0.05. Proportional data were analyzed using a Generalized linear model (GLM) with binomial distribution and combined with Tukey's *post-hoc* test for pairwise comparisons. The data on hemocyte numbers were analyzed using a negative binomial GLM followed by pairwise comparisons of groups using estimated marginal means. A Kruskal-Wallis rank sum test combined with Dunn's *post hoc* test was applied to GFP intensity comparisons in **Figure 3D**. R version 4.0.4 was used to perform GLM and Kruskal-Wallis rank sum tests.

RESULTS

Potential Interaction Partners of Eye Transformer (ET) Analyzed by Mass Spectrometry

In a previous study, we used a large-scale RNAi screen in *Drosophila* S2 cells to discover genes important for the *Drosophila* JAK/STAT pathway (31). In the screen we identified Eye transformer (ET) as a negative regulator of the JAK/STAT pathway (31). To screen for putative ET interactors, we created a *Drosophila* S2 cell-line stably overexpressing the ET protein with a V5 tag (ET-V5), and affinity-purified all the proteins in the ET complex with the V5 antibody. In **Supplementary Figure 1A**, it is shown that the ET-V5 signal can be detected with the V5-antibody (α-V5) in the lysates from ET-V5-expressing S2 cells. Since this control experiment showed that ET-V5 is successfully captured with this method, we next affinity purified proteins in complex with ET, separated them using SDS-PAGE and visualized the proteins by silver staining (**Supplementary Figure 1B**). Each line was cut, digested with trypsin and the protein composition was determined by mass spectrometry.

The potential ET interaction partners were studied in two situations, either with or without overexpression of the Dome receptor ligand *upd1*. When the ligand is present, the JAK/STAT pathway is activated, whereas without the ligand, the pathway stays inactive. In addition, untreated S2 cells and S2 cells transfected with an empty pMT vector were used as negative controls. After proteins that were also found in the negative controls were excluded, we identified in total 173 *Drosophila melanogaster* proteins in complex with ET under the conditions where the JAK/STAT pathway was inactive (ET-V5 alone) and 175 proteins when the ligand Upd1 was present (ET-V5 + *Upd1-myc*). Out of these, 136 proteins were found in both situations (ET with and without Upd1 induction). The mass spectrometry raw data, including putative candidates for JAK/STAT pathway regulation, is shown in **Supplementary Table 2**.

The Proteasome Complex Components Negatively Regulate JAK/STAT Pathway Activation in S2 Cells

The mass spectrometry screen identified in total 212 unique putative interaction partners of ET (**Supplementary Table 2**). These genes/proteins were compared to the Kallio & coworker’s screen for JAK/STAT components (31) as well as other literature, to search for links to the JAK/STAT pathway, including immunity, hematopoiesis or stress response (25). In total, nine genes were selected for further study: four gene products where the interaction was detected with ET alone, three gene products where the interaction with ET was detected upon Upd1 induction and two gene products where the interaction was detected with ET both with and without Upd1 induction. The selected genes are listed in **Table 1**, with a description of the gene function deduced from the www.flybase.org gene pages. To assess if the association of ET with these nine gene products signifies a regulatory effect on the JAK/STAT pathway, we carried out a JAK/STAT pathway reporter assay in S2 cells with dsRNAs targeting the genes (**Figure 1A**). As shown in **Figure 1A**, induction with overexpression of either *upd1* (gray bars) or *hop^{Tum-1}* (black bars) causes an activation of the

JAK/STAT pathway, as assessed by the production of the luciferase signal from the JAK/STAT target gene luciferase reporter construct *Turandot M-luciferase (TotM-luc)*. GFP dsRNA was used as a negative control in both assays. Knockdown of *ET* was used as a positive control in measuring the Upd1-induced *TotM-luc* activity, but as *ET* is upstream of Hop, its knockdown does not have an increasing effect on Hop^{Tum-1}-induced *TotM-luc* activity, but instead, a decreasing effect, as discussed e.g., in (31). Of the nine RNAi treatments tested, only *Proteasome α 6 subunit (Pro α 6)* causes hyperactivation of the JAK/STAT pathway upon *hop^{Tum-1}* induction. Pro α 6 is a component of the core particle of the proteasome complex [see below (43)]. The Upd1-induced *TotM-luc* signal is enhanced when *G protein α o subunit (G α)*, *Myosin light chain cytoplasmic (Mlc-c)*, *Moesin (Moe)*, *Pro α 6* or *Twins (tws)* are knocked down by targeted RNAi.

We have previously carried out a genome-wide JAK/STAT pathway RNAi screen (31), and when analyzing unpublished putative negative regulators of the pathway found in the screen, we identified 16 genes whose RNAi caused more than a 10-fold hyperactivation of the JAK/STAT pathway (**Table 2** and **Figure 1B**). Of these, 69% (11/16) had a described function in the proteasome pathway. The five non-proteasome-related putative negative regulator genes, are *hephaestus (heph)*, *karyopherin α 3 (Kap- α 3)*, *Furin1 (Fur1)*, *Integrator 2 (IntS2)* and *Integrator 6 (IntS6)*.

The proteasome is a large protein complex consisting of a 20S core particle capped by 19S regulatory particles (43). Among the seven alpha rings of the proteasome core particle, RNAi-mediated silencing of *Pro α 1*, *Pro α 6* and *Pro α 7* caused hyperactivation of the JAK/STAT pathway as did silencing of four of the seven beta ring sub-particles and one related gene, namely *Pro β 2*, *Pro β 3*, *Pro β 5*, *Pro β 7* and *Pro β 2R1*. Moreover, silencing of the *Drosophila* 19S regulatory particle genes *Rpn1*, *Rpn2* and *Rpn3*, as well as proteasome-related chaperone protein *Pomp*, had similar effects (**Table 2** and **Figure 1B**). In conclusion, RNAi-mediated silencing of the expression of proteasome genes causes hyperactivation of the JAK/STAT pathway in S2 cells [**Table 2** and **Figure 1B** (44)].

TABLE 1 | Selected putative ET interaction partners from the mass spectrometry study.

CG number	Gene name	Symbol	Description
Interaction detected with ET alone:			
CG11804	<i>ced-6</i>	<i>ced-6</i>	intracellular adaptor protein, involved in signal transduction (phagocytosis of apoptotic cells)
CG2204	<i>G protein α o subunit</i>	<i>Gα</i>	involved in signaling by a variety of GPCRs
CG2849	<i>Ras-like protein A</i>	<i>Rala</i>	GTPase known to regulate Notch, JAK/STAT and JNK signaling pathways
CG6235	<i>Twins</i>	<i>tws</i>	regulatory subunit of protein phosphatase 2A
Interaction detected with ET upon Upd induction:			
CG10060	<i>G protein α i subunit</i>	<i>Gai</i>	G protein α subunit, sequence homology to mammalian Gi α that inhibits adenylate cyclase activity
CG3201	<i>Myosin light chain cytoplasmic</i>	<i>Mlc-c</i>	subunit of the myosin complex, involved in actin filament-based movement
CG10701	<i>Moesin</i>	<i>Moe</i>	involved in cortical cytoskeleton stability, regulates the products of <i>crb</i> and <i>Rho</i> 1
Interaction detected with ET both with and without Upd induction:			
CG7425	<i>Effete</i>	<i>eff</i>	conserved class I E2 ubiquitin-conjugating enzyme, protein ubiquitination and degradation pathway
CG4904	<i>Proteasome α6 subunit</i>	<i>Proα6</i>	Proteasome 35kD subunit, endopeptidase activity, orthologous to human PSMA1 (proteasome 20S subunit alpha 1).

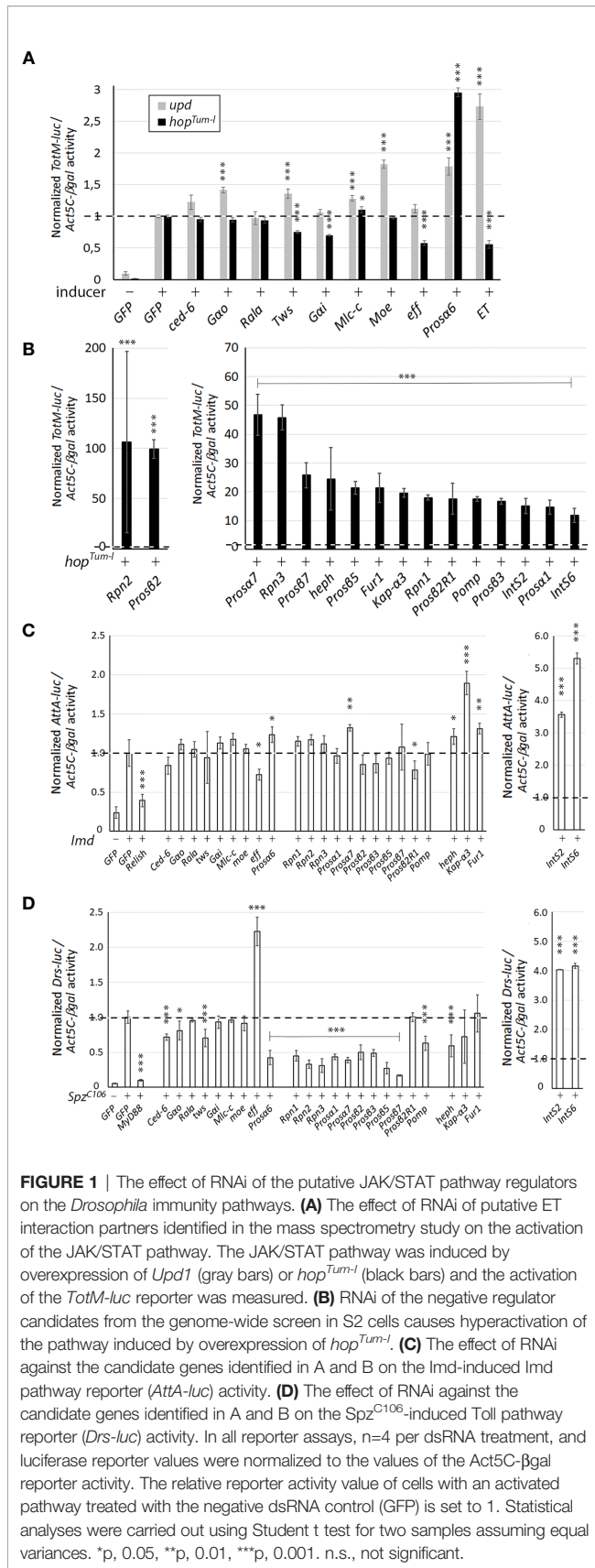


FIGURE 1 | The effect of RNAi of the putative JAK/STAT pathway regulators on the *Drosophila* immunity pathways. **(A)** The effect of RNAi of putative ET interaction partners identified in the mass spectrometry study on the activation of the JAK/STAT pathway. The JAK/STAT pathway was induced by overexpression of *Upd1* (gray bars) or *hop^{Tum-1}* (black bars) and the activation of the *TotM-luc* reporter was measured. **(B)** RNAi of the negative regulator candidates from the genome-wide screen in S2 cells causes hyperactivation of the pathway induced by overexpression of *hop^{Tum-1}*. **(C)** The effect of RNAi against the candidate genes identified in A and B on the Imd-induced Imd pathway reporter (*AtTA-luc*) activity. **(D)** The effect of RNAi against the candidate genes identified in A and B on the *Spz^{C106}*-induced Toll pathway reporter (*Drs-luc*) activity. In all reporter assays, n=4 per dsRNA treatment, and luciferase reporter values were normalized to the values of the Act5C-βgal reporter activity. The relative reporter activity value of cells with an activated pathway treated with the negative dsRNA control (GFP) is set to 1. Statistical analyses were carried out using Student t test for two samples assuming equal variances. *p, 0.05, **p, 0.01, ***p, 0.001. n.s., not significant.

The Effect of RNAi-Mediated Silencing of the Putative JAK/STAT Pathway Regulators on the Activity of the Imd and Toll Pathways

The total of twenty-five genes from the study of ET interaction partners (Table 1 and Figure 1A) and from the Kallio & coworkers' RNAi screen for negative regulators of the JAK/STAT pathway (Table 2 and Figure 1B (31), were selected for further study. To investigate if these genes act in the regulation of other immune-related pathways besides JAK/STAT, we tested if their silencing affects the activation of the Imd or Toll pathways using reporter assays. To investigate effects on the Imd pathway, the pathway was induced by transfecting S2 cells with the Imd plasmid and relevant dsRNAs. *GFP* was used as a negative control and *Relish* dsRNA as a positive control. As shown in Figure 1C, most of the genes studied do not regulate the Imd pathway; however, knockdown of *effete* (*eff*) and *Proso2R1* leads to a slight decrease in pathway activation compared to *GFP*. *Effete*, the *Drosophila* homolog of the Ubc5 E2-ubiquitin conjugating enzyme, has previously been shown to be needed for Imd ubiquitination (45). Knockdown of *Proso6*, *Proso7*, *heph* and *Fur1* leads to a slight elevation in the Imd pathway activation, whereas when *Kap-α3*, *IntS2*, and *IntS6* are silenced, the pathway is markedly upregulated (Figure 1C).

To investigate the effects of silencing of the selected 25 genes on the Toll pathway, the pathway was induced by overexpression of the *Spz^{C106}* plasmid. A *MyD88* dsRNA treatment was used as a positive and *GFP* as a negative control of the pathway. As shown in Figure 1D, the silencing of several genes resulted in a reduction in Toll pathway activity, including mainly components of the proteasome: *Rpn*-genes, *Pomp*, *Prosoα*- and *Prosoβ*-genes (but not *Proso2R1*). A statistically significant reduction was seen also with *Ced-6*, *Gao*, *Twins* (*tw5*) and *heph*. Three genes that negatively regulate the Toll pathway were identified: *IntS2*, *IntS6* and *eff*. The effect of *IntS2* and *IntS6* on the Toll pathway has been previously shown (46), but the effect of *eff* on the Toll pathway has not been previously studied and remains to be investigated.

As a summary, the integrator complex members (*IntS2* and *IntS6*) appear to negatively regulate all pathways tested indicating that their effect is not specific to the JAK/STAT pathway. Although *Effete* co-localizes with ET, it does not seem to regulate the *TotM-luc* reporter gene activation mediated by the JAK/STAT pathway. Instead, *Effete* appears to negatively regulate the Toll pathway in S2 cells, which requires further exploration in the future. RNAi against the proteasome complex components does not have major effects on the Imd pathway, but silencing proteasome complex members decreases the activity of the Toll pathway indicating that the proteasome positively regulates the Toll pathway. Cactus, the *Drosophila* homologue of the mammalian Inhibitor of κB (IκB), is known to be degraded by the proteasome upon induction of the Toll pathway (47, 48), so it is plausible that silencing components of the proteasome complex leads to accumulation of the Cactus protein and reduction in the activity of the Toll pathway also in this context.

TABLE 2 | JAK/STAT pathway negative regulators from the genome-wide RNAi screen (cut off FC = 10), grouped by function.

CG number	Name	Symbol	Description	Human ortholog
Members of the 26S proteasome complex, components of the 19S regulatory particle				
CG7762	Regulatory particle non-ATPase 1	Rpn1	zinc ion binding, enzyme regulator activity	
CG11888	Regulatory particle non-ATPase 2	Rpn2	zinc ion binding, enzyme regulator activity	PSMD1 ⁽¹⁾
CG10484/CG42641	Regulatory particle non-ATPase 3	Rpn3	zinc ion binding, enzyme regulator activity	PSMD3 ⁽¹⁾
Members of the 26S proteasome complex, components of the 20S core particle, α subunits (outer rings)				
CG18495	Proteasome α1 subunit	Prosα1	predicted endopeptidase activity	PSMA6 ⁽²⁾
CG1519	Proteasome α7 subunit	Prosα7	predicted endopeptidase activity	PSMA3 ⁽²⁾
Members of the 26S proteasome complex, components of the 20S core particle, β subunits (inner rings)				
CG3329	Proteasome β2 subunit	Prosβ2	predicted endopeptidase activity	PSMB7 ⁽³⁾
CG11981	Proteasome β3 subunit	Prosβ3	predicted endopeptidase activity	PSMB3 ⁽³⁾
CG12323	Proteasome β5 subunit	Prosβ5	predicted endopeptidase activity	PSMB5/PSMB8 ⁽³⁾
CG12000	Proteasome β7 subunit	Prosβ7	predicted endopeptidase activity	PSMB4 ⁽³⁾
CG18341	Proteasome β2 subunit-related 1	Prosβ2R1	predicted endopeptidase activity	PSMB7 ⁽³⁾
Other, proteasome-related				
CG9324	Pomp	Pomp	A chaperone protein, incorporation of 20S core particle β subunits	POMP ⁽⁴⁾
Other, not proteasome-related				
CG31000	hephaestus	heph	nucleo-cytoplasmic shuttling protein, involved in Notch signaling regul.	PTBP1/PTBP2/PTBP3 ⁽⁵⁾
CG9423	karyopherin-alpha3	Kap-α3	Notch binding, myosin binding, prot. Nucl. Import	KPNA3/KPNA4 ⁽⁶⁾
CG10772	Furin1	Fur1	serine-type endopeptidase activity, plasma membrane	FURIN
CG8211	Integrator 2	IntS2	component of the Integrator complex	INTS2 ⁽⁷⁾
CG3125	Integrator 6	IntS6	component of the Integrator complex	INTS6/INTS6L ⁽⁷⁾

⁽¹⁾PSMD = proteasome 26S subunit non-ATPase.

⁽²⁾PSMA = proteasome 20S subunit alpha.

⁽³⁾PSMB = proteasome 20S subunit beta.

⁽⁴⁾POMP = proteasome maturation protein.

⁽⁵⁾PTBP = polypyrimidine tract binding protein.

⁽⁶⁾KPNA = karyopherin subunit alpha.

⁽⁷⁾INTS = integrator complex subunit.

Prosα6 Silencing Leads to Reduced Expression of ET and Reduced Amounts of the ET Protein

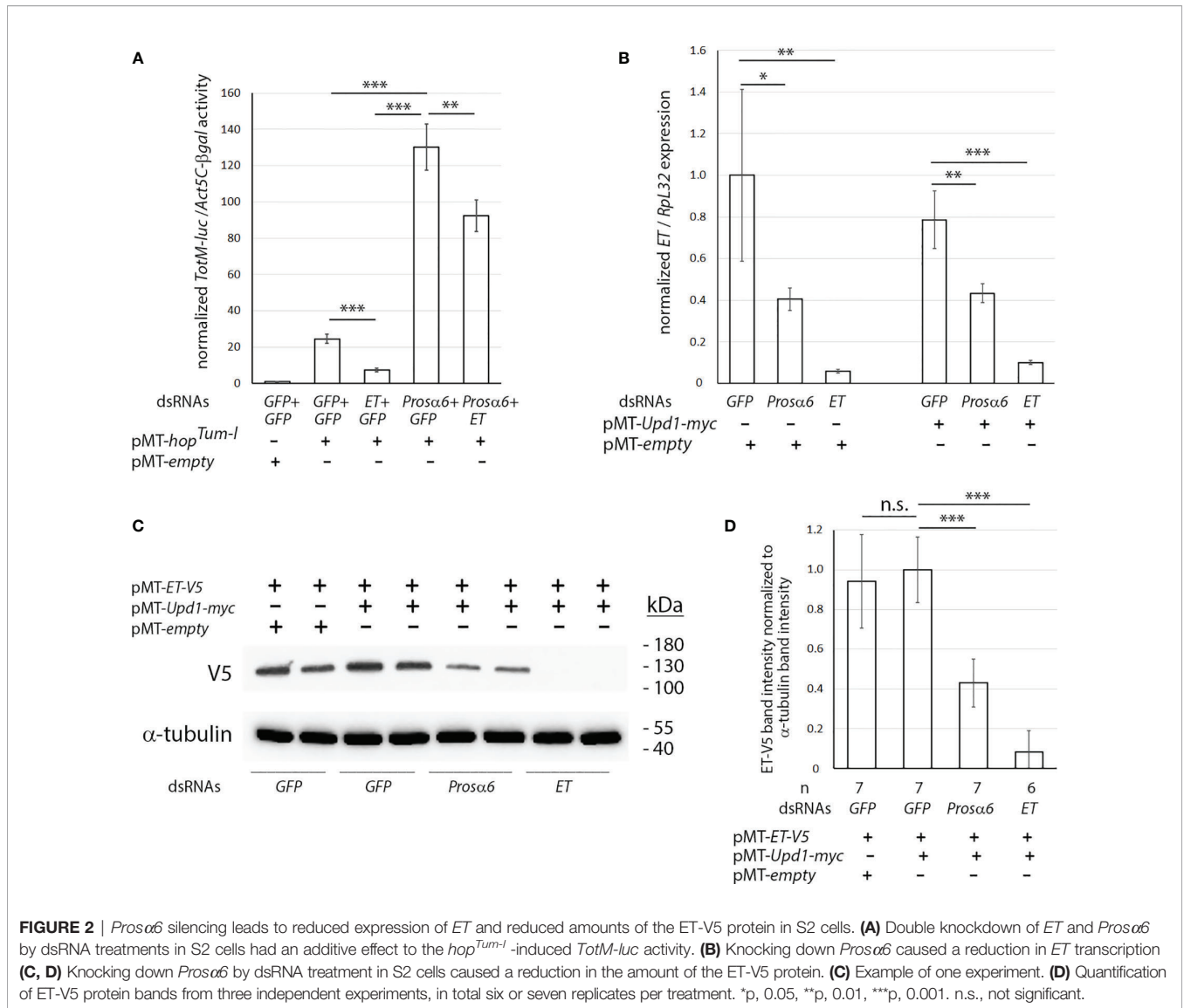
Because the proteasomal genes were identified in JAK/STAT pathway regulation in S2 cells (Figures 1A, B), we selected Prosα6 to study in more detail. To study the interplay between ET and Prosα6 in the JAK/STAT pathway, we carried out a double knockdown experiment with ET and Prosα6. As shown in Figure 2A, the TotM-luc activity was induced with the pMT-hop^{Tum-1} construct. As previously shown, ET knockdown reduces this hop^{Tum-1}-induced TotM-luc activity [(31) and Figure 1A], while Prosα6 knockdown causes hyperactivation of this activity (Figure 1A). When both ET and Prosα6 are knocked down simultaneously (Prosα6+ET), the result is additive, indicating that the effect of ET and Prosα6 proteins on the JAK/STAT pathway activation is partially independent.

Next, we investigated what happens to the expression of ET upon Prosα6 knockdown. S2 cells were treated with Prosα6 dsRNA and control dsRNAs and either transfected with pMT-Upd1-myc, which induces the JAK/STAT pathway, or transfected with the pMT-empty plasmid for control. ET expression values from RNAs extracted from the cells were measured and normalized with RpL32 expression. As shown in Figure 2B, Prosα6 knockdown causes reduction in the transcription of ET

both in conditions where the JAK/STAT pathway is inactive, and in those where it is activated with overexpression of Upd1.

Further, we investigated the effect of Prosα6 knockdown on the amount of ET protein, by treating S2 cells with Prosα6 dsRNA and control dsRNAs and transfecting them with pMT-ET-V5 together with pMT-Upd1-myc, which induces the JAK/STAT pathway. Treatment of cells with the pMT-empty vector and GFP dsRNA was used as a control. Cellular lysates were prepared and subjected to SDS-PAGE electrophoresis, Western blotting and antibody treatments and imaged. The ET-V5 protein band intensity was normalized to α-tubulin band intensity values in each sample. As shown in Figures 2C, D, the amount of ET-V5 protein is reduced in Prosα6 dsRNA-treated cell lysates compared to the negative control GFP dsRNA-treated lysates. Figure 2C shows an example of one experiment, and Figure 2D shows the quantification from three independent experiments including in total six or seven replicates per treatment. In ET dsRNA-treated cells, the ET-V5 band is not at all visible indicating that RNAi in S2 cells silences the protein production of the targeted gene very efficiently.

In conclusion, upon knockdown of Prosα6, ET transcription as well as the amount of the ET protein is decreased. As ET is the key negative regulator of the JAK/STAT pathway, these results in part explain the hyperactivation of the pathway by knockdown of Prosα6.



Prosα6 Silencing in Hemocytes Activates JAK/STAT Signaling

Since our previous results indicated involvement of the proteasome complex in regulating JAK/STAT signaling in S2 cells, we next tested if this was also the case *in vivo* in *Drosophila* larval hemocytes. We used a STAT reporter *10xSTAT92E-GFP* combined with a hemocyte driver *He-GAL4* as a read-out of the JAK/STAT activity in hemocytes using flow cytometry. As a positive control we overexpressed a constitutively active *Drosophila* JAK/STAT pathway component *hopscotch* (*hop*) in hemocytes (*10xStat92E-GFP;He-GAL4/UAS-hop^{Tum-1}*), and as expected, detected an increase in the *Stat92E-GFP* signal compared to control hemocytes. We also detected a clear increase in the reporter expression when knocking down the *Proteasome α6 subunit* (*10xStat92E-GFP;He-GAL4/UAS-Prosα6^{GD}*) compared to control hemocytes expressing only the reporter (**Figure 3A**).

The FSC-area (FSC-A) vs. FSC-height (FSC-H) plot is often used to exclude cell doublets from further flow cytometry analysis taking advantage of the fact that round particles will appear as a population at a 45° angle, while doublets have larger area than height. We observed that while the control animals had mainly round hemocytes (plasmatocytes) (49), appearing at a 45° angle in the FSC-A vs. FSC-H plot, *Prosα6* silencing resulted in cells detected outside of this area, similar to when *hop^{Tum-1}* was overexpressed in hemocytes (**Figure 3B**). Overexpression of *hop^{Tum-1}* is known to cause hematopoietic neoplasia leading to the formation of melanotic nodules and a specific hemocyte type, the lamellocyte (6, 42). Furthermore, Avet-Rochex and coworkers (50) identified *Prosα6* (then called *Pros35*) as a suppressor of melanotic nodules in *Drosophila* larval hemocytes. Therefore, we reasoned that at least a fraction of these hemocytes outside the 45° area might be lamellocytes, which, due to their flat and discoidal morphology (49), fall outside the area where the round plasmatocytes are detected in

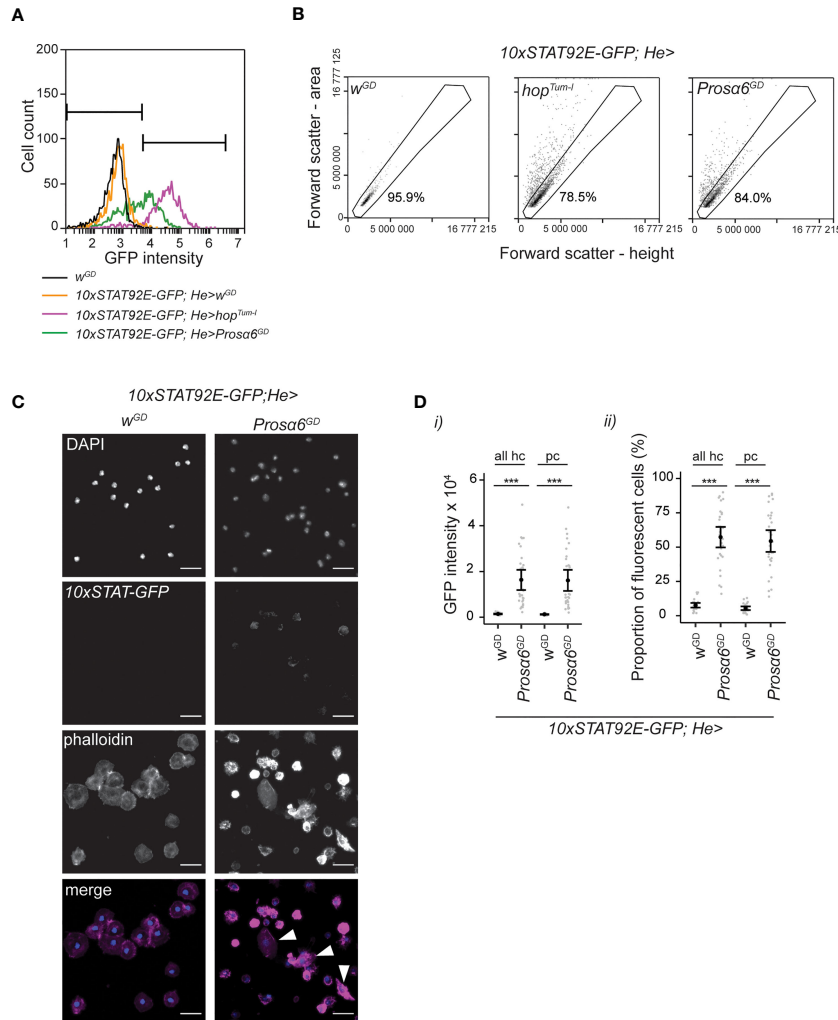


FIGURE 3 | *Prosa6* silencing in hemocytes activates JAK/STAT signaling. **(A)** Examples of GFP fluorescence intensity in non-fluorescent (w^{GD} , black line), control (orange line), hop^{Tum-I} overexpressing (purple line) and in *Prosa6* knockdown (green line) hemocytes. Note that in the figures the symbol “>” denotes the presence of the GAL4/UAS system. The genotypes for control, hop^{Tum-I} overexpressing and *Prosa6* knockdown animals are $10xSTAT92E-GFP;He-GAL4/w^{GD}$, $10xSTAT92E-GFP;He-GAL4/UAS-hop^{Tum-I}$ and $10xSTAT92E-GFP;He-GAL4/UAS-Prosa6^{GD}$, respectively. Bars mark GFP-negative (on the left) and GFP-positive (on the right) areas. **(B)** Hemocytes detected in $10xSTAT92E-GFP;He-GAL4/w^{GD}$, $10xSTAT92E-GFP;He-GAL4/UAS-hop^{Tum-I}$ and $10xSTAT92E-GFP;He-GAL4/UAS-Prosa6^{GD}$ animals in forward scatter area vs. height plot. While in the controls (w^{GD}) most cells resided at a 45° angle in the area vs. height plot, the *Prosa6* knockdown and hop^{Tum-I} overexpressing animals had hemocytes deviating from this area. Gated area represents hemocytes that are considered round (mainly non-activated plasmatocytes). Percentages represent the hemocytes falling into this gate in these example plots. 822 control, 2119 hop^{Tum-I} overexpression and 1857 *Prosa6* knockdown cells were analyzed for **(A, B)**. **(C)** Fluorescence microscopy of hemocytes from the control and *Prosa6* knockdown larvae expressing the 10xSTAT-GFP and stained with the nuclear stain DAPI and the F-actin stain Phalloidin. Hemocytes with lamellocyte morphology (marked with arrowheads) were found in *Prosa6* knockdown larvae but not in controls. Of note, DAPI staining appears dimmer in the *Prosa6* knockdown sample, but this was likely due to slide-to-slide variation. Scale bars 10 μ m. **(D)** Quantification of 10xSTAT-GFP signal intensity and percentage of fluorescent hemocytes in controls and in the *Prosa6* knockdown animals. All hc, the whole hemocyte population; pc, hemocytes inside the gate shown in **(B)**. Hemocytes were analyzed from two replicates of w^{GD} (nine animals each) and three replicates of *Prosa6*^{GD} (10 animals each), comprising of an order of 10⁴ cells in each replicate. Error bars show mean and lower and upper confidence limits (cl). Grey dots represent individual animals. ***p < 0.001. Intensity values were analyzed using a Kruskal-Wallis rank sum test combined with Dunn’s *post hoc* test. The proportions of fluorescent cells were analyzed using a GLM with binomial distribution combined with Tukey’s *post-hoc* test.

the control animals. Since lamellocytes can be easily separated from plasmatocytes by morphology, we stained hemocytes from $10xStat92E-GFP;He-GAL4/UAS-Prosa6^{GD}$ and $10xStat92E-GFP;He-GAL4/w^{GD}$ 3rd instar larvae with the F-actin stain Phalloidin to visualize hemocyte morphology. We found that hemocytes from the *Prosa6* knockdown larvae had more variation in their

morphology when compared to the control hemocytes and observed the presence of hemocytes with a lamellocyte morphology (**Figure 3C**).

Next, we analyzed the GFP signal intensity of the *Stat92E-GFP* reporter and the proportion of fluorescent hemocytes separately in all hemocytes and in the plasmatocyte fraction

(Figure 3B). In both cases, the GFP signal was significantly higher in the hemocytes where *Prosα6* was silenced compared to controls (Figure 3D, i). Also, the fraction of GFP-positive hemocytes increased significantly in both populations after *Prosα6* knockdown (Figure 3D, ii). These data indicate that silencing *Prosα6* leads to activation of JAK/STAT signaling also *in vivo*.

Silencing *Prosα6* in Hemocytes Leads to Activation of Hemocytes and Differentiation of an Infection-Induced Hemocyte Type, the Lamellocyte

Prompted by the observation of the appearance of lamellocytes and JAK/STAT reporter activation after *Prosα6* silencing in hemocytes, we studied the hemocyte phenotype further. To investigate if silencing of *Prosα6* in hemocytes causes hemocyte differentiation, we utilized hemocyte reporter constructs *eaterGFP* (expressed in plasmatocytes) and *msnCherry* (expressed in lamellocytes) combined with the *Hml^A-GAL4* and *He-GAL4* to silence *Prosα6* in hemocytes and to quantify hemocyte types using a flow cytometer. Flow cytometry analysis of hemocytes showed that while in a wild-type larva, the majority of the hemocyte pool consists of *eaterGFP*-positive plasmatocytes, the silencing of *Prosα6* caused aberrant lamellocyte differentiation and hemocyte activation (Figure 4A, i-iii). The hemocyte response was stronger with the *UAS-Prosα6^{GD}* construct, where the numbers of all identified hemocyte types were increased, including lamelloblasts, the putative lamellocyte precursors, and prelamellocytes (Figure 4B, i-vi). A similar, but milder, response was seen also with the *UAS-Prosα6^{KK}* construct. Furthermore, around 25% of *Hml^A-GAL4;He-GAL4/UAS-Prosα6^{GD}* larvae exhibited melanotic nodules, while in *Hml^A-GAL4;He-GAL4/UAS-Prosα6^{KK}* larvae this phenotype was again milder (Figure 4C, i-ii).

Since silencing *Prosα6* in hemocytes led to hemocyte activation and melanotic nodule formation at the larval stage, we further studied the effects of *Prosα6* silencing on egg-to-adult development and the lifespan of the flies. We found that while egg-to-pupal development of the animals with *Prosα6* silencing in hemocytes was comparable to the controls (Supplementary Figure 2A), the pupal eclosion rate was lower in animals expressing *UAS-Prosα6^{GD}* in hemocytes, whereas animals expressing *UAS-Prosα6^{KK}* eclosed at a normal rate (Supplementary Figure 2A). Inspection of the pupal cases revealed melanotic nodules in a fraction of animals with *Prosα6* silencing (1% in *msnCherry,eaterGFP;Hml^A-GAL4;He-GAL4//UAS-Prosα6^{KK}* and 20% in *msnCherry,eaterGFP;Hml^A-GAL4;He-GAL4//UAS-Prosα6^{GD}*; Supplementary Figure 2B), similar to the levels observed in larvae (Figure 4C). The lifespan of the *msnCherry,eaterGFP;Hml^A-GAL4;He-GAL4/UAS-Prosα6^{GD}* flies, both males and females, was shorter than that of the control flies, whereas the lifespan of *msnCherry,eaterGFP;Hml^A-GAL4;He-GAL4/UAS-Prosα6^{KK}* flies was not affected (Supplementary Figures 2C, D). When the expression of *Prosα6* normalized to *RpL32* was measured from hemocytes

by qRT-PCR, it was shown that in the *Hml^A-GAL4;He-GAL4/UAS-Prosα6^{GD}* hemocytes, *Prosα6* expression was $43 \pm 14\%$ from the respective control (*w/Prosα6^{GD}*), whereas in the *Hml^A-GAL4;He-GAL4/UAS-Prosα6^{KK}* hemocytes, *Prosα6* expression was $52 \pm 17\%$ from the control (*w/UAS-Prosα6^{KK}*) hemocytes (Supplementary Figure 2E).

To conclude, knocking down *Prosα6* in hemocytes causes immune activation characterized by the differentiation and activation of hemocytes and the formation of melanotic nodules, but also decreases the viability of the flies. It is possible that there is a threshold level of silencing needed for the full phenotypic effects, as with the KK line, only the mild activation of hemocytes, but not the other phenotypes, is seen.

JAK/STAT and JNK Signaling Are Needed for the Full Hemocyte Activation Caused by *Prosα6* Silencing

To further verify that *Prosα6* silencing induces hemocyte activation *via* JAK/STAT signaling, we opted for a genetic rescue experiment. We knocked down *Prosα6* using the GD construct simultaneously with *Stat92E* and checked the effect on the hemocyte phenotype. Since also the JNK pathway has been shown to be important in lamellocyte formation (6), we also tested whether it has a role in hemocyte activation in the *Prosα6* silencing background. To this end, we knocked down *Prosα6* simultaneously with *hemipterous (hep)*, a *Drosophila* JNK-pathway component and checked the hemocyte composition. Knocking down *Stat92E* alone in hemocytes resulted in a mild activating effect; a small number of lamelloblasts and lamellocytes were detected in an otherwise wild type background (Figure 5A). Knocking down *hep* led to a reduction in total hemocyte numbers compared to the control (Figure 5B). Neither *Stat92E* nor *hep* knockdown in the *Prosα6*-silenced background led to the rescue of total hemocytes, or of plasmatocytes, lamelloblasts or activated plasmatocytes, back to the levels detected in the control animals (Figures 5A, B, i-iv). Both, however, reduced the formation of prelamellocytes and lamellocytes induced by *Prosα6* silencing (Figures 5A, B, v-vi). Even though knocking down neither *Stat92E* nor *hep* in the *Prosα6* background rescued the hemocyte phenotype completely to the wild-type levels, the number of lamellocytes produced by the *Prosα6* knockdown (600 on average) was reduced approximately seven-fold with *Stat92E* knock-down (51) and four-fold with *hep* knockdown (148). Taken together, these results suggest that *Prosα6* silencing-induced hemocyte activation requires the function of the JAK/STAT pathway, and that the JNK pathway functions in parallel or downstream of JAK/STAT eliciting hemocyte activation.

DISCUSSION

In this study we have investigated the potential interaction partners of ET, and other putative regulators of the JAK/STAT pathway using our previously unpublished RNAi screen data. Among the 25 genes that were selected for further study, 12 have

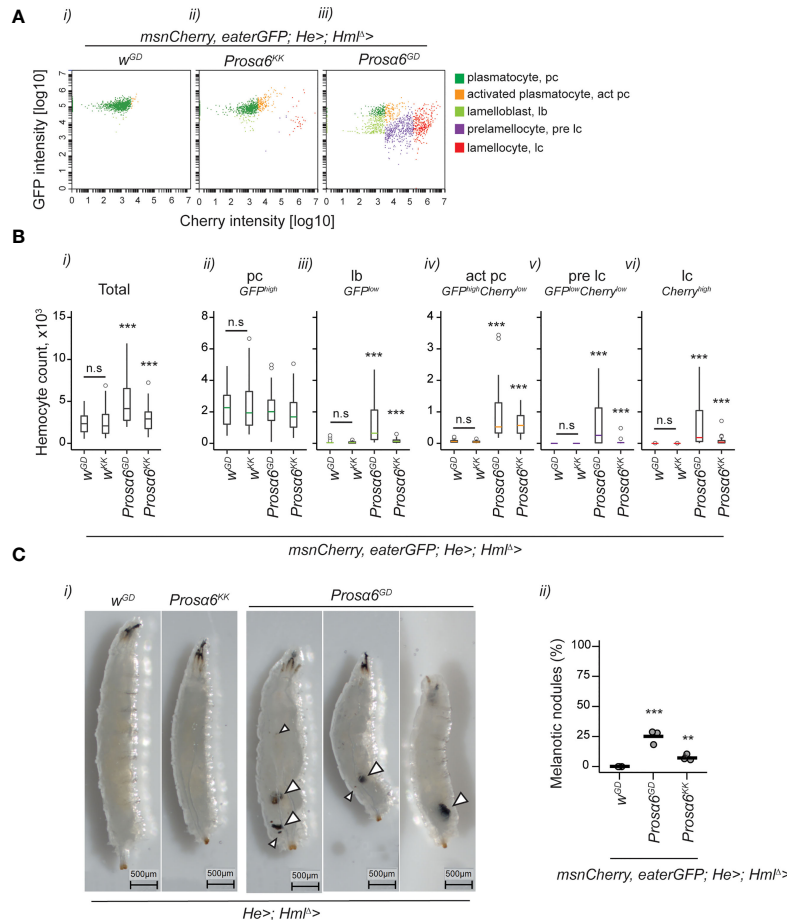


FIGURE 4 | *Prosα6* silencing in hemocytes leads to an increase in total hemocyte numbers and to the formation of activated hemocytes. **(A)** Examples of flow cytometry plots showing hemocytes expressing *eaterGFP* (a plasmatocyte marker) and *msnCherry* (a lamellocyte marker). A wild-type larva had mainly *eaterGFP*-positive plasmatocytes (i), whereas *Prosα6* silencing in hemocytes (*msnCherry,eaterGFP;Hml^Δ-GAL4;He-GAL4/UAS-Prosα6*) resulted in the formation of lamellocytes (ii) or a full-blown activation of hemocytes (iii). **(B)** Quantification of total hemocytes (i) and each hemocyte class (ii-vi) from control (*msnCherry,eaterGFP;Hml^Δ-GAL4;He-GAL4/w^{SD}* and *msnCherry,eaterGFP;Hml^Δ-GAL4;He-GAL4/w^{KK}*) larvae and from larvae with *Prosα6* silencing in hemocytes (*msnCherry,eaterGFP;Hml^Δ-GAL4;He-GAL4/UAS-Prosα6^{GD}* and *msnCherry,eaterGFP;Hml^Δ-GAL4;He-GAL4/UAS-Prosα6^{KK}*). Each genotype was replicated three times, 10 animals in each replicate. Error bars show mean and lower and upper 95% confidence limits (ci). Grey dots represent individual animals. Data on hemocytes were analyzed using a negative binomial GLM. Stars indicate a significant difference when compared to the control sample. The two control backgrounds were also compared to each other. n.s., not significant; ***p < 0.001; pc, plasmatocyte; act pc, activated plasmatocyte; lb, lamelloblast; pre lc, prelamellocyte; lc, lamellocyte. **(C)** i) Examples of larvae without and with melanotic hemocyte aggregates of varying sizes, some of which are marked with arrowheads. For nodule quantification, each genotype was replicated three times, with 100 animals in each replicate (ii). Data were analyzed as a proportion of animals bearing nodules, using a GLM with binomial distribution combined with Tukey's *post-hoc* test. ***p < 0.001; **p < 0.01.

a described function in the proteasome pathway. These were *Rpn1*, *Rpn2*, *Rpn3*, *Prosa1*, *Prosa6*, *Prosa7*, *Prosβ2*, *Prosβ3*, *Prosβ5*, *Prosβ7*, *Prosβ2R1* and *Pomp*, all of which caused elevation of *TotM-luc* activity upon activation of the JAK/STAT pathway by *hop^{Tum-1}* in S2 cells. The 26S proteasome is a large complex composed of many subunits and under normal conditions, it degrades most proteins in the cell (52). It is known that the half-life of a protein varies from minutes to months, but at some point, every protein is marked and brought to degradation. In eukaryotes, unwanted proteins are marked for proteasomal degradation mainly with K48-linked polyubiquitin chains (53), which are recognized by the proteasome 19S regulatory particle. The regulatory particle functions in binding

the ubiquitinated target proteins and deubiquitinating, unfolding and translocating them to the 20S proteasome core particle for cleavage (43). The core particle is a barrel shaped structure containing two outer rings each formed by seven α-subunits, and two inner rings formed by seven β-subunits. The β-subunits create a chamber where the proteolytically active sites are located. The N-termini of α-subunits form a gate that lets the substrates (target proteins) in through the central α-ring channel (52).

The ubiquitin-proteasome pathway has been implicated in the regulation of the JAK/STAT pathway in mammals: treatment with proteasome inhibitors prolongs the activation of the JAK/STAT pathway in response of many cytokine stimuli, e.g (54–

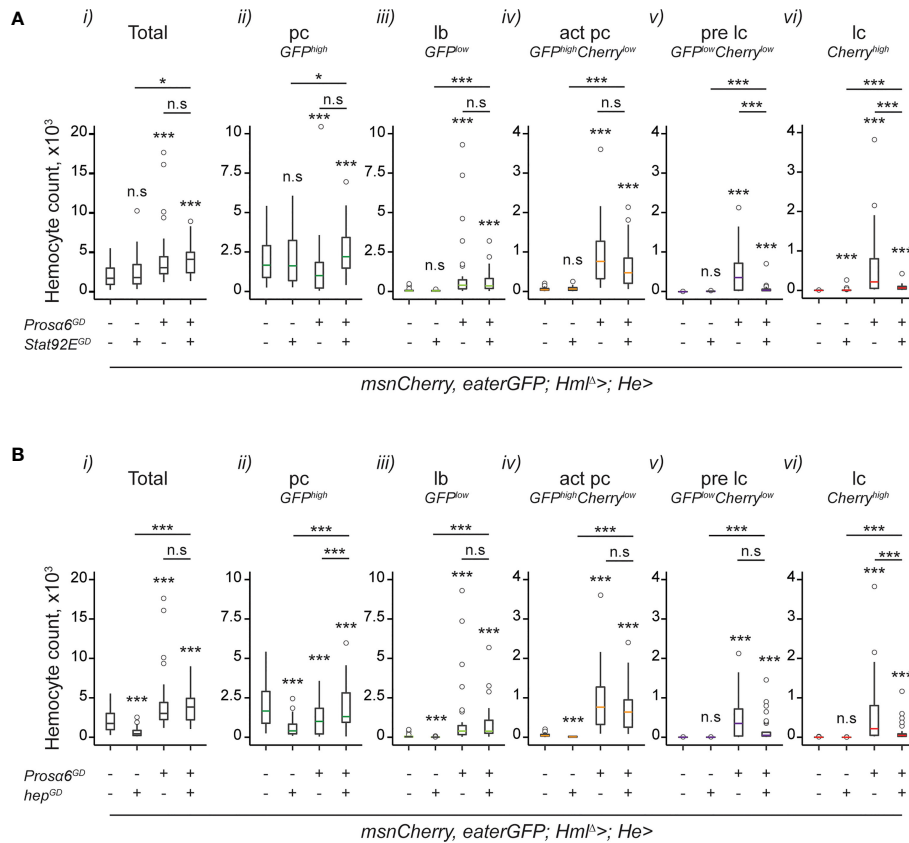


FIGURE 5 | Knocking down JAK/STAT and JNK pathway components in the *Prosα6* background reduce the hemocyte activation caused by the *Prosα6* silencing. **(A)** Effects of JAK/STAT pathway component *Stat92E* knockdown on *Prosα6*-induced hemocyte phenotype. i) Total hemocyte counts. ii-vi) Differential hemocyte counts. “-/+” indicate the presence of *Prosα6* and *Stat92E* knockdowns. Stars refer to the statistical difference compared to the wild-type control larvae (*msnCherry, eaterGFP; Hml^Δ-GAL4; He-GAL4/w^{GD}*), the first sample in each plot. Underlined stars refer to the statistical difference of the simultaneous knockdown of *Prosα6* and *Stat92E* (*msnCherry, eaterGFP; Hml^Δ-GAL4; He-GAL4/UAS-Prosα6^{GD}; UAS-Stat92E^{GD}*) to the single knockdowns of *Prosα6* (short line) and *Stat92E* (longer line). **(B)** Effects of JNK pathway component *hep* knockdown on *Prosα6*-induced hemocyte phenotype. i) Total hemocyte counts. ii-vi) Differential hemocyte counts. “-/+” indicate the presence of *Prosα6* and *hep* knockdowns. Stars refer to the statistical difference compared to the wild-type control larvae (*msnCherry, eaterGFP; Hml^Δ-GAL4; He-GAL4/w^{GD}*), the first sample in each plot. Underlined stars refer to the statistical difference of the simultaneous knockdown of *Prosα6* and *hep* (*msnCherry, eaterGFP; Hml^Δ-GAL4; He-GAL4/UAS-Prosα6^{GD}; UAS-hep^{GD}*) to the single knockdowns of *Prosα6* (short line) and *hep* (longer line). Each genotype was replicated three times, except for the *msnCherry, eaterGFP; Hml^Δ-GAL4; He-GAL4/w^{GD}* control, which was replicated 6 times, 10 animals in each replicate. Note that the control and *Prosα6* hemocyte data is the same in **(A, B)** and has been plotted separately for clarity. Statistical analyses have been conducted on the whole dataset and p-values adjusted according to multiple comparisons. Data was analyzed using a negative binomial GLM. n.s., not significant; *p < 0.05; ***p < 0.001; pc, plasmatocyte; lb, lamelloblast; pre lc, prelamellocyte; lc, lamellocyte.

56). The mechanisms of proteasome-related regulation of the JAK/STAT pathway are complex: treatment with proteasome inhibitors causes stabilization of tyrosine-phosphorylated forms of STAT1 (56), STAT4, STAT5, STAT6 (57) and Jak2 (58), and thereby prolonged JAK/STAT activation. Furthermore, treatment with proteasome inhibitors also causes stabilization of the complex of the Jak2 protein with SOCS-1 (Suppressor Of Cytokine Signaling-1); SOCS-1 expression would normally enhance the proteasomal degradation of Jak2, but when the proteasome function is blocked, the Jak2/SOCS-1 complexes accumulate (58). So in mammals, the SOCS proteins (eight proteins, SOCS-1-7 and CIS) (59) bring another layer to the regulation of the JAK/STAT pathway. The *Drosophila* JAK/STAT pathway has similar core pathway components as mammals, but there is less redundancy. For instance, in

Drosophila, three members of the SOCS family have been identified, out of which Socs36E appears to be the main negative regulator of the pathway (25, 60). Similarities have been found also in the regulation of the *Drosophila* and mammalian JAK/STAT pathways, such as between the *Drosophila* non-signaling receptor/inhibitor ET and the mammalian gp130, the soluble form of which can inhibit signaling (25, 31, 61).

We show that the knockdown of the *Proteasome α6 subunit* results in reduction in *ET* transcription, and reduction in the amount of the ET protein in *Drosophila* S2 cells (31). It appears that *Prosα6* expression is needed for full *ET* expression to prevent aberrant activation of the JAK/STAT pathway. This regulation may be very complex: for example, *Prosα6* knockdown, i.e., inhibition of the normal proteasome function, may cause an accumulation of

other regulatory protein(s) causing a reduction in *ET* expression. The reduction mechanism appears to inhibit ET production already at the transcriptional level, and this effect is seen in both basal conditions and in conditions, where the JAK/STAT pathway is activated.

Moreover, we show that silencing *Pro α 6* in *Drosophila* hemocytes *in vivo* and thereby blocking the proteasomal degradation/turn-over step leads to overactivation of JAK/STAT signaling, aberrant activation of immune cells and the formation of clusters of activated immune cells, known as melanotic nodules or pseudotumors. Our findings are in line with an earlier *in vivo* RNAi screen conducted by Avet-Rochex & coworkers (50), who looked for genes involved in blood cell homeostasis in *Drosophila*. In the screen, they identified *Pro α 6* (*Pros35*) as a suppressor of melanotic nodules in hemocytes. Moreover, we show that there is partial rescue of the *Pro α 6* knockdown-induced hemocyte activation phenotype not only with knockdown of *STAT92E*, but also *hemipterous* (*hep*), the Jun-kinase in *Drosophila*. These results may indicate that the pathways act synergistically, both being needed for full hemocyte activation. For example, the JNK and JAK/STAT pathways act in cooperation in the wing imaginal disc resulting in the loss of cell fate specification as a response to damage (62). Alternatively, it has been shown that the JAK/STAT ligands *upd1-3* are transcriptional targets of the JNK pathway (63). Therefore, it is possible that the silencing of the JNK pathway leads to reduced *upd* expression, and hence has a dampening effect on the overall activity of the JAK/STAT signaling in hemocytes. So, in addition to the JAK/STAT pathway activation, the JNK pathway seems to be needed for full blown hemocyte activation brought upon by *Pro α 6* silencing, but the exact mechanism of this interaction remains to be elucidated.

The proteasome has also been shown to be involved in the turn-over and regulation of several key proteins in immune signaling. On the one hand, proteasomal degradation of inhibitory molecules such as the Inhibitor of κ B (I κ B) is essential for pathway activation (64) but on the other hand, shutting down un-needed immune activation is equally important, and proteasomal degradation of key factors is one such regulatory mechanism (58, 65). In *Drosophila*, it has been shown that the proteasome represses the Imd pathway, probably by causing the degradation of Relish (NF- κ B factor in the *Drosophila* Imd pathway) (66). Here we show that the proteasome is needed for proper Toll pathway activity, likely because Cactus (*Drosophila* I κ B in the Toll pathway) has to be degraded upon pathway activation (47, 48).

In addition to proteasome-related genes, we identified additional genes that interact with ET and/or affect the JAK/STAT activity (*G α* , *G α i*, *Mlc-c*, *Moe*, *tws*, *eff*, *Fur*, *heph*, *Kap- α 3*, *IntS2* and *IntS6*). Importantly, the effect of a specific knockdown was dependent on the means of the pathway activation. Silencing of two out of eight genes studied with both inducers (*Upd1* and *Hop^{Tum-1}*) resulted in a change on the *TotM-luc* reporter expression with both inducers: *Mlc-c* (to the same direction) and *tws* (to opposite directions). *Mlc-c* forms an essential light chain of Non-muscle myosin II, which is involved in shaping the actin cytoskeleton of cells in e.g., development (67). Since JAK/STAT functions in the control of

myogenic differentiation (68), it might be that in this case the activation of the signaling pathway is in response to reduced levels of myosin II. *Drosophila tws* encodes a regulatory B/PR55 subunit of protein phosphatase 2A (PP2A), and it has been shown to play a role in e.g., cell division, tissue patterning and multiple signaling pathways (69, 70). In human T-cell lines, inhibition of PPA2 has been shown to attenuate at least STAT3, STAT5 and STAT6 function (71–73), and there is some indication that it may act similarly in *Drosophila* neuroblasts (74).

Silencing of all the rest of the genes appeared to affect the JAK/STAT signaling activity only in a specific induction context. It is also possible that in some cases, the lack of significant effect may be due to insufficient silencing of the corresponding genes, since in this screen for putative interactors, we only tested one dsRNA per gene. *G α* and *G α i* belong to the conserved family of the heterotrimeric G protein α subunits, which act as effector molecules of G-protein coupled receptors (GPCRs) (75). Both *G α* and *G α i* were found to activate STAT3 in a murine fibroblast cell line (76, 77), whereas we found that knockdown of *G α* enhanced the *Upd1*-induced JAK/STAT pathway activity and knock-down of *G α i* reduced the *Hop^{Tum-1}*-induced JAK/STAT. Moesin is a member of the FERM domain (band 4.1, Ezrin, Radixin and Moesin), which is also one of the protein domains at the N-terminus of Jaks enabling the adaptor and scaffolding interactions (78, 79). Similarly in *Drosophila*, moesin is a member of the FERM protein domain, and is an important factor in processes including cell adhesion, cell movement and membrane trafficking (51).

The ubiquitin-conjugating enzymes function in mediating a variety of ubiquitin modifications, including the K48-linked polyubiquitination that directs the ubiquitinated proteins for degradation by the 26S proteasome (80) as well as K63-linked activating polyubiquitination events (45, 81). *Eff* is an E2 ubiquitin-conjugating enzyme, and it has previously been shown to be needed for the K63-linked polyubiquitination of the cleaved Imd molecule for functional Imd signaling (45). Similarly to the Imd pathway, *eff* knockdown has a positive regulatory effect on the *Hop^{Tum-1}*-induced JAK/STAT pathway in S2 cells. On the other hand, our results indicate that *Eff* negatively regulates the Toll pathway in S2 cells, but it appears not to be needed in the fat body mediated defense *in vivo*. Furins are a family of evolutionarily conserved serine endoprotease enzymes that cleave precursor proteins into their mature forms (82). In accordance with our results, silencing of *Drosophila Fur1* in the fat body has previously been shown to elevate the transcription of stress response genes including the JAK/STAT pathway target gene *TotM* (83).

The Notch signaling pathway is well conserved from flies to humans and has been shown to be essential for blood cell development and lineage speciation (11, 84). *Kap- α 3* (also called importin- α 3) has been shown to be required for regulating Notch signaling (85) and *Heph* has been shown to be an important protein regulating Notch signaling in wing development (86). Both *Kap- α 3* and *Heph* negatively regulate the *Hop^{Tum-1}*-induced JAK/STAT pathway in S2 cells indicating interplay between the Notch and JAK/STAT signaling pathways in this context. The integrator complex genes, in turn, have been suggested to have multiple

functions: the main function of the complex is to mediate the 3' processing of small nuclear RNAs (87). In addition, silencing of the zebrafish Integrator 5 or 11 has been shown to result in defects in hematopoiesis; this was suggested to be due to misprocessing of snRNA, which leads to splicing defects in the mRNA of genes required for hematopoiesis (88). We show that silencing of *IntS2* and *IntS6*, members of the *Drosophila* Integrator complex, results in an increase in the activity of the JAK/STAT pathway. The integrator complex has previously also been shown to negatively regulate the Toll pathway (46).

We also identified proteins that did interact with ET but did not affect JAK/STAT activity in our S2 assay (*Rala* and *ced-6*). *Rala*, which belongs to the family of Ras-like (Ral) small GTPases homologous to $G\alpha$ -proteins, is shown to be required cell-autonomously in regulating polar-cell specific markers, including the JAK/STAT pathway ligand Upd, in the developing oocyte (89). Although associating in the complex with ET, it appears that in the S2-cell context, *Rala* knockdown affects neither the Upd1 nor the Hop^{Tum-1}-induced activity of the JAK/STAT pathway. *Ced-6* has been identified as an essential adaptor protein for apoptotic clearance of unneeded cells by hemocytes in the developing embryo (90) as well as phagocytosis of *S. aureus* gram-positive bacteria in *Drosophila* adults upon infection (91). It has not previously been implicated in the regulation of JAK/STAT signaling to our knowledge.

The JAK/STAT signaling pathway, like many other signaling pathways, has core and tissue/cell type specific signaling outcomes (92, 93). Accordingly, also the regulatory events outside the core pathway components might vary among the cell types. Our data revealed several putative JAK/STAT regulators in S2 cells, whose mode of action was often dependent on the way the pathway was activated. Importantly, silencing of the proteasome complex member *Pro α 6* consistently enhanced the JAK/STAT pathway activity. Moreover, knockdown of *Pro α 6* is sufficient to induce the activation of *Drosophila* blood cells, the hemocytes, *in vivo*, via a JAK/STAT pathway-dependent mechanism. The interplay between the *Drosophila* JAK/STAT pathway components and negative regulators including ET and the proteasome appears complex and remains to be further explored in detail.

DATA AVAILABILITY STATEMENT

The original contributions presented in the study are included in the article/**Supplementary Material**. Further inquiries can be directed to the corresponding author.

REFERENCES

- Vigano S, Perreau M, Pantaleo G, Harari A. Positive and Negative Regulation of Cellular Immune Responses in Physiologic Conditions and Diseases. *Clin Dev Immunol* (2012) 2012:485781. doi: 10.1155/2012/485781
- Horwitz DA, Fahmy TM, Piccirillo CA, La Cava A. Rebalancing Immune Homeostasis to Treat Autoimmune Diseases. *Trends Immunol* (2019) 40:888–908. doi: 10.1016/j.it.2019.08.003
- Baeg GH, Zhou R, Perrimon N. Genome-Wide Rnai Analysis of JAK/STAT Signaling Components in *Drosophila*. *Genes Dev* (2005) 19:1861–70. doi: 10.1101/gad.1320705
- Cokic VP, Mitrovic-Ajtic O, Beleslin-Cokic BB, Markovic D, Buac M, Diklic M, et al. Proinflammatory Cytokine IL-6 and JAK-STAT Signaling Pathway in Myeloproliferative Neoplasms. *Mediators Inflamm* (2015) 2015:453020. doi: 10.1155/2015/453020
- O'Sullivan JM, Harrison CN. JAK-STAT Signaling in the Therapeutic Landscape of Myeloproliferative Neoplasms. *Mol Cell Endocrinol* (2017) 451:71–9. doi: 10.1016/j.mce.2017.01.050
- Zettervall CJ, Anderl I, Williams MJ, Palmer R, Kurucz E, Ando I, et al. A Directed Screen for Genes Involved in *Drosophila* Blood Cell Activation. *Proc Natl Acad Sci USA* (2004) 101:14192–7. doi: 10.1073/pnas.0403789101

AUTHOR CONTRIBUTIONS

MJ-S, LV, MR, and SV designed the experiments. MJ-S, MM, JC, and SV carried out the *in vitro* S2 cell experiments. LV, MJ-S, and SV performed the *in vivo* larval hemocyte experiments. All authors analyzed their own data. LV, MJ-S, MR, and SV wrote the paper. All authors contributed to the article and approved the submitted version.

FUNDING

This work was supported by the Tampere University Doctoral Programme in Medicine and Life Sciences and The Finnish Cultural Foundation (to MJ-S); The Sigrid Juselius Foundation, the Academy of Finland (Grant 277495), the Competitive State Research Financing of the Expert Responsibility Area of Oulu University Hospital and the Tampere Tuberculosis Foundation (to MR); and the Tuberculosis foundation (to SV). The Tampere *Drosophila* Facility, the Tampere Imaging Facility and the Tampere Facility of Flow Cytometry are all partially funded by Biocenter Finland.

ACKNOWLEDGMENTS

We thank Tuula Myllymäki and Tea Tuomela (Tampere University, Finland) for technical assistance with the fly work and Dr Ines Anderl for the *yw, msnF9mo-mCherry, eaterGFP; Hml Δ -GAL4; He-GAL4* fly line. We thank Tuula Nyman (University of Helsinki, Finland) for helping with the mass spectrometry analysis. All fly work was carried out in the Tampere *Drosophila* Facility. We also acknowledge the Tampere Imaging Facility (TIF) and the Tampere Facility of Flow Cytometry for the service. We thank all the members of the Experimental Immunology research group and members of the Tampere *Drosophila* community for insightful scientific as well as methodological discussions.

SUPPLEMENTARY MATERIAL

The Supplementary Material for this article can be found online at: <https://www.frontiersin.org/articles/10.3389/fimmu.2021.729631/full#supplementary-material>

7. Luo H, Rose PE, Roberts TM, Dearolf CR. The Hopscotch Jak Kinase Requires the Raf Pathway to Promote Blood Cell Activation and Differentiation in *Drosophila*. *Mol Genet Genomics* (2002) 267:57–63. doi: 10.1007/s00438-001-0632-7
8. Minakhina S, Steward R. Melanotic Mutants in *Drosophila*: Pathways and Phenotypes. *Genetics* (2006) 174:253–63. doi: 10.1534/genetics.106.061978
9. Vlisidou I, Wood W. *Drosophila* Blood Cells and Their Role in Immune Responses. *FEBS J* (2015) 282:1368–82. doi: 10.1111/febs.13235
10. Meister M, Lagueux M. *Drosophila* Blood Cells. *Cell Microbiol* (2003) 5:573–80. doi: 10.1046/j.1462-5822.2003.00302.x
11. Evans CJ, Hartenstein V, Banerjee U. Thicker Than Blood: Conserved Mechanisms in *Drosophila* and Vertebrate Hematopoiesis. *Dev Cell* (2003) 5:673–90. doi: 10.1016/S1534-5807(03)00335-6
12. Markus R, Laurinyecz B, Kurucz E, Honfi V, Bajusz I, Sipos B, et al. Sessile Hemocytes as a Hematopoietic Compartment in *Drosophila Melanogaster*. *Proc Natl Acad Sci USA* (2009) 106:4805–9. doi: 10.1073/pnas.0801766106
13. Makhijani K, Alexander B, Tanaka T, Rulifson E, Bruckner K. The Peripheral Nervous System Supports Blood Cell Homing and Survival in the *Drosophila* Larva. *Development* (2011) 138:5379–91. doi: 10.1242/dev.067322
14. Brehelin M. Comparative Study of Structure and Function of Blood Cells From Two *Drosophila* Species. *Cell Tissue Res* (1982) 221:607–15. doi: 10.1007/BF00215704
15. Tepass U, Fessler LI, Aziz A, Hartenstein V. Embryonic Origin of Hemocytes and Their Relationship to Cell Death in *Drosophila*. *Development* (1994) 120:1829–37. doi: 10.1242/dev.120.7.1829
16. Rizki TM, Rizki RM. Lamellocyte Differentiation in *Drosophila* Larvae Parasitized by Leptopilina. *Dev Comp Immunol* (1992) 16:103–10. doi: 10.1016/0145-305X(92)90011-Z
17. Williams MJ. *Drosophila* Hemopoiesis and Cellular Immunity. *J Immunol* (2007) 178:4711–6. doi: 10.4049/jimmunol.178.8.4711
18. Galko MJ, Krasnow MA. Cellular and Genetic Analysis of Wound Healing in *Drosophila* Larvae. *PLoS Biol* (2004) 2:E239. doi: 10.1371/journal.pbio.0020239
19. Rämet M, Lanot R, Zachary D, Manfrulli P. JNK Signaling Pathway is Required for Efficient Wound Healing in *Drosophila*. *Dev Biol* (2002) 241:145–56. doi: 10.1006/dbio.2001.0502
20. Hanratty WP, Ryerse JS. A Genetic Melanotic Neoplasm of *Drosophila Melanogaster*. *Dev Biol* (1981) 83:238–49. doi: 10.1016/0012-1606(81)90470-X
21. Zoranovic T, Grmai L, Bach EA. Regulation of Proliferation, Cell Competition, and Cellular Growth by the *Drosophila* JAK-STAT Pathway. *JAKSTAT* (2013) 2:e25408. doi: 10.4161/jkst.25408
22. Harrison DA. The Jak/STAT Pathway. *Cold Spring Harbor Perspect Biol* (2012) 4:a011205. doi: 10.1101/cshperspect.a011205
23. Hou XS, Melnick MB, Perrimon N. Marelle Acts Downstream of the *Drosophila* HOP/JAK Kinase and Encodes a Protein Similar to the Mammalian Stats. *Cell* (1996) 84:411–9. doi: 10.1016/s0092-8674(00)81286-6
24. Binari R, Perrimon N. Stripe-Specific Regulation of Pair-Rule Genes by Hopscotch, a Putative Jak Family Tyrosine Kinase in *Drosophila*. *Genes Dev* (1994) 8:300–12. doi: 10.1101/gad.8.3.300
25. Myllymäki H, Rämet M. JAK/STAT Pathway in *Drosophila* Immunity. *Scand J Immunol* (2014) 79:377–85. doi: 10.1111/sji.12170
26. Vanha-aho LM, Valanne S, Rämet M. Cytokines in *Drosophila* Immunity. *Immunol Lett* (2016) 170:42–51. doi: 10.1016/j.imlet.2015.12.005
27. Zeidler MP, Bausek N. The *Drosophila* JAK-STAT Pathway. *JAKSTAT* (2013) 2:e25353. doi: 10.4161/jkst.25353
28. Amoyel M, Anderson AM, Bach EA. JAK/STAT Pathway Dysregulation in Tumors: A *Drosophila* Perspective. *Semin Cell Dev Biol* (2014) 0:96–103. doi: 10.1016/j.semcdb.2014.03.023
29. Hombria JC, Brown S. The Fertile Field of *Drosophila* Jak/STAT Signalling. *Curr Biol* (2002) 12:569. doi: 10.1016/s0960-9822(02)01057-6
30. Arbouzova NI, Zeidler MP. JAK/STAT Signalling in *Drosophila*: Insights Into Conserved Regulatory and Cellular Functions. *Development* (2006) 133:2605–16. doi: 10.1242/dev.02411
31. Kallio J, Myllymäki H, Grönholm J, Armstrong M, Vanha-aho LM, Makinen L, et al. Eye Transformer Is a Negative Regulator of *Drosophila* JAK/STAT Signaling. *FASEB J* (2010) 24:4467–79. doi: 10.1096/fj.10-162784
32. Makki R, Meister M, Pennetier D, Ubuda JM, Braun A, Daburon V, et al. A Short Receptor Downregulates JAK/STAT Signalling to Control the *Drosophila* Cellular Immune Response. *PLoS Biol* (2010) 8:e1000441. doi: 10.1371/journal.pbio.1000441. 10.1371/journal.pbio.1000441.
33. Kleino A, Valanne S, Ulvila J, Kallio J, Myllymäki H, Enwald H, et al. Inhibitor of Apoptosis 2 and TAK1-Binding Protein Are Components of the *Drosophila* Imd pathway. *EMBO J* (2005) 24:3423–34. doi: 10.1038/sj.emboj.7600807
34. Valanne S, Myllymäki H, Kallio J, Schmid MR, Kleino A, Murumagi A, et al. Genome-Wide RNA Interference in *Drosophila* Cells Identifies G Protein-Coupled Receptor Kinase 2 as a Conserved Regulator of NF-κB Signaling. *J Immunol* (2010) 184:6188–98. doi: 10.4049/jimmunol.1000261
35. Välimäki E, Miettinen JJ, Lietzen N, Matikainen S, Nyman TA. Monosodium Urate Activates Src/Pyk2/PI3 Kinase and Cathepsin Dependent Unconventional Protein Secretion From Human Primary Macrophages. *Mol Cell Proteomics* (2013) 12:749–63. doi: 10.1074/mcp.M112.024661
36. Brand AH, Perrimon N. Targeted Gene Expression as a Means of Altering Cell Fates and Generating Dominant Phenotypes. *Development* (1993) 118:401–15. doi: 10.1242/dev.118.2.401
37. Sorrentino RP, Tokusumi T, Schulz RA. The Friend of GATA Protein U-Shaped Functions as a Hematopoietic Tumor Suppressor in *Drosophila*. *Dev Biol* (2007) 311:311–23. doi: 10.1016/j.ydbio.2007.08.011
38. Tokusumi T, Sorrentino RP, Russell M, Ferrarese R, Govind S, Schulz RA. Characterization of a Lamellocyte Transcriptional Enhancer Located Within the *Missshapen* Gene of *Drosophila Melanogaster*. *PLoS One* (2009) 4:e6429. doi: 10.1371/journal.pone.0006429
39. Sinenko SA, Mathey-Prevot B. Increased Expression of *Drosophila* Tetraspanin, Tsp68C, Suppresses the Abnormal Proliferation of Ytr-Deficient and Ras/Raf-Activated Hemocytes. *Oncogene* (2004) 23:9120–8. doi: 10.1038/sj.onc.1208156
40. Bach EA, Ekas LA, Ayala-Camargo A, Flaherty MS, Lee H, Perrimon N, et al. GFP Reporters Detect the Activation of the *Drosophila* JAK/STAT Pathway *In Vivo*. *Gene Expr Patterns* (2007) 7:323–31. doi: 10.1016/j.modgep.2006.08.003
41. Harrison DA, Binari R, Nahreini TS, Gilman M, Perrimon N. Activation of a *Drosophila* Janus Kinase (JAK) Causes Hematopoietic Neoplasia and Developmental Defects. *EMBO J* (1995) 14:2857–65. doi: 10.1002/j.1460-2075.1995.tb07285.x
42. Anderl I, Vesala L, Ihalainen TO, Vanha-aho LM, Ando I, Rämet M, et al. Transdifferentiation and Proliferation in Two Distinct Hemocyte Lineages in *Drosophila Melanogaster* Larvae After Wasp Infection. *PLoS Pathog* (2016) 12:e1005746. doi: 10.1371/journal.ppat.1005746
43. Tomko JR Jr, Hochstrasser M. Molecular Architecture and Assembly of the Eukaryotic Proteasome. *Annu Rev Biochem* (2013) 82:415–45. doi: 10.1146/annurev-biochem-060410-150257
44. Yu CL, Burakoff SJ. Involvement of Proteasomes in Regulating Jak-STAT Pathways Upon Interleukin-2 Stimulation. *J Biol Chem* (1997) 272:14017–20. doi: 10.1074/jbc.272.22.14017
45. Paquette N, Broemer M, Aggarwal K, Chen L, Husson M, Ertürk-Hasdemir D, et al. Caspase-Mediated Cleavage, IAP Binding, and Ubiquitination: Linking Three Mechanisms Crucial for *Drosophila* NF-κB Signaling. *Mol Cell* (2010) 37:172–82. doi: 10.1016/j.molcel.2009.12.036
46. Valanne S, Järvelä-Stölting M, Harjula SE, Myllymäki H, Salminen TS, Rämet M. Osa-Containing Brahma Complex Regulates Innate Immunity and the Expression of Metabolic Genes in *Drosophila*. *J Immunol* (2020) 204:2143–55. doi: 10.4049/jimmunol.1900571
47. Belvin MP, Anderson KV. A Conserved Signaling Pathway: The *Drosophila* Toll-Dorsal Pathway. *Annu Rev Cell Dev Biol* (1996) 12:393–416. doi: 10.1146/annurev.cellbio.12.1.393
48. Daigneault J, Klemetsaune L, Wasserman SA. The IRAK Homolog Pelle Is the Functional Counterpart of IκB Kinase in the *Drosophila* Toll Pathway. *PLoS One* (2013) 8:e75150. doi: 10.1371/journal.pone.0075150
49. Rizki TM, Rizki RM. Properties of the Larval Hemocytes of *Drosophila Melanogaster*. *Experientia* (1980) 36:1223–6. doi: 10.1007/BF01976142
50. Avet-Rochex A, Boyer K, Polesello C, Gobert V, Osman D, Roch F, et al. An *In Vivo* RNA Interference Screen Identifies Gene Networks Controlling *Drosophila Melanogaster* Blood Cell Homeostasis. *BMC Dev Biol* (2010) 10:65. doi: 10.1186/1471-213X-10-65
51. Vilmos P, Jankovics F, Szathmári M, Lukácsovich T, Henn L, Erdélyi M. Live Imaging Reveals That the *Drosophila* Actin-Binding ERM Protein, Moesin, Co-Localizes With the Mitotic Spindle. *Eur J Cell Biol* (2009) 88:609–19. doi: 10.1016/j.ejcb.2009.05.006
52. Budenholzer L, Cheng CL, Li Y, Hochstrasser M. Proteasome Structure and Assembly. *J Mol Biol* (2017) 429:3500–24. doi: 10.1016/j.jmb.2017.05.027

53. Grice GL, Nathan JA. The Recognition of Ubiquitinated Proteins by the Proteasome. *Cell Mol Life Sci* (2016) 73:3497–506. doi: 10.1007/s00018-016-2255-5
54. Callus BA, Mathey-Prevot B. Interleukin-3–Induced Activation of the JAK/STAT Pathway Is Prolonged by Proteasome Inhibitors. *Blood* (1998) 91:3182–92. doi: 10.1182/blood.V91.9.3182
55. Verdier F, Walrafen P, Hubert N, Chretien S, Gisselbrecht S, Lacombe C, et al. Proteasomes Regulate the Duration of Erythropoietin Receptor Activation by Controlling Down-Regulation of Cell Surface Receptors. *J Biol Chem* (2000) 275:18375–81. doi: 10.1074/jbc.275.24.18375
56. Kim TK, Maniatis T. Regulation of Interferon-Gamma-Activated STAT1 by the Ubiquitin-Proteasome Pathway. *Science* (1996) 273:1717–9. doi: 10.1126/science.273.5282.1717
57. Wang D, Moriggl R, Stravopodis D, Carpino N, Marine JC, Teglund S, et al. A Small Amphipathic Alpha-Helical Region Is Required for Transcriptional Activities and Proteasome-Dependent Turnover of the Tyrosine-Phosphorylated Stat5. *EMBO J* (2000) 19:392–9. doi: 10.1093/emboj/19.3.392
58. Ungureanu D, Saharinen P, Junttila I, Hilton DJ, Silvennoinen O. Regulation of Jak2 Through the Ubiquitin-Proteasome Pathway Involves Phosphorylation of Jak2 on Y1007 and Interaction With SOCS-1. *Mol Cell Biol* (2002) 22:3316–26. doi: 10.1128/MCB.22.10.3316-3326.2002
59. Linossi EM, Calleja DJ, Nicholson SE. Understanding SOCS Protein Specificity. *Growth Factors* (2018) 36:104–17. doi: 10.1080/08977194.2018.1518324
60. Stec W, Vidal O, Zeidler MP. *Drosophila* SOCS36E Negatively Regulates JAK/STAT Pathway Signaling via Two Separable Mechanisms. *Mol Biol Cell* (2013) 24:3000–9. doi: 10.1091/mbc.E13-05-0275
61. Narazaki M, Yasukawa K, Saito T, Ohsugi Y, Fukui H, Koishihara Y, et al. Soluble Forms of the Interleukin-6 Signal-Transducing Receptor Component Gp130 in Human Serum Possessing a Potential to Inhibit Signals Through Membrane-Anchored Gp130. *Blood* (1993) 82:1120–6. doi: 10.1182/blood.V82.4.1120.1120
62. Ahmed-de-Prado S, Diaz-Garcia S, Baonza A. JNK and JAK/STAT Signalling Are Required for Inducing Loss of Cell Fate Specification During Imaginal Wing Discs Regeneration in *Drosophila Melanogaster*. *Dev Biol* (2018) 441:31–41. doi: 10.1016/j.ydbio.2018.05.021
63. Kucinski I, Dinan M, Kolahgar G, Piddini E. Chronic Activation of JNK/JAK/STAT and Oxidative Stress Signalling Causes the Loser Cell Status. *Nat Commun* (2017) 8:136. doi: 10.1038/s41467-017-00145-y
64. Scherer DC, Brockman JA, Chen Z, Maniatis T, Ballard DW. Signal-Induced Degradation of I Kappa B Alpha Requires Site-Specific Ubiquitination. *PNAS* (1995) 92:11259–63. doi: 10.1073/pnas.92.24.11259
65. Wertz IE, Dixit VM. Signaling to NF-kb: Regulation by Ubiquitination. *Cold Spring Harb Perspect Biol* (2010) 2:a003350. doi: 10.1101/cshperspect.a003350
66. Khush RS, Cornwell WD, Uram JN, Lemaître B. A Ubiquitin-Proteasome Pathway Represses the *Drosophila* Immune Deficiency Signaling Cascade. *Curr Biol* (2002) 12:1728–37. doi: 10.1016/S0960-9822(02)01214-9
67. Aldaz S, Escudero LM, Freeman M. Dual Role of Myosin II During *Drosophila* Imaginal Disc Metamorphosis. *Nat Commun* (2013) 4:1761. doi: 10.1038/ncomms2763
68. Jang Y, Baik EJ. JAK-STAT Pathway and Myogenic Differentiation. *JAKSTAT* (2013) 2:e23282. doi: 10.4161/jkst.23282
69. Shi Y. Serine/Threonine Phosphatases: Mechanism Through Structure. *Cell* (2009) 139:468–84. doi: 10.1016/j.cell.2009.10.006
70. Janssens V, Goris J. Protein Phosphatase 2A: A Highly Regulated Family of Serine/Threonine Phosphatases Implicated in Cell Growth and Signalling. *Biochem J* (2001) 353:417–39. doi: 10.1042/0264-6021:3530417
71. Woetmann A, Brockdorff J, Lovato P, Nielsen M, Leick V, Rieneck K, et al. Protein Phosphatase 2A (PP2A) Regulates Interleukin-4-Mediated STAT6 Signaling. *J Biol Chem* (2003) 278:2787–91. doi: 10.1074/jbc.M210196200
72. Woetmann A, Nielsen M, Christensen ST, Brockdorff J, Kaltoft K, Engel AM, et al. Inhibition of Protein Phosphatase 2A Induces Serine/Threonine Phosphorylation, Subcellular Redistribution, and Functional Inhibition of STAT3. *Proc Natl Acad Sci USA* (1999) 96:10620–5. doi: 10.1073/pnas.96.19.10620
73. Ross JA, Cheng H, Nagy ZS, Frost JA, Kirken RA. Protein Phosphatase 2A Regulates Interleukin-2 Receptor Complex Formation and JAK3/STAT5 Activation. *J Biol Chem* (2010) 285:3582–91. doi: 10.1074/jbc.M109.053843
74. Chabu C, Doe CQ. Twins/PP2A Regulates Apkc to Control Neuroblast Cell Polarity and Self-Renewal. *Dev Biol* (2009) 330:399–405. doi: 10.1016/j.ydbio.2009.04.014
75. Milligan G, Kostenis E. Heterotrimeric G-Proteins: A Short History. *Br J Pharmacol* (2006) 147:S46–55. doi: 10.1038/sj.bjp.0706405
76. Corre I, Baumann H, Hermouet S. Regulation by Gi2 Proteins of V-Fms-Induced Proliferation and Transformation via Src-Kinase and STAT3. *Oncogene* (1999) 18:6335–42. doi: 10.1038/sj.onc.1203010
77. Ram PT, Horvath CM, Iyengar R. Stat3-Mediated Transformation of NIH-3T3 Cells by the Constitutively Active Q205L Galphao Protein. *Science* (2000) 287:142–4. doi: 10.1126/science.287.5450.142
78. Haan S, Margue C, Engrand A, Rolvering C, Schmitz-Van de Leur H, Heinrich PC, et al. Dual Role of the Jak1 FERM and Kinase Domains in Cytokine Receptor Binding and in Stimulation-Dependent Jak Activation. *J Immunol* (2008) 180:998–1007. doi: 10.4049/jimmunol.180.2.998
79. Seif F, Khoshmirsafa M, Aazami H, Mohsenzadegan M, Sedighi G, Bahar M. The Role of JAK-STAT Signaling Pathway and Its Regulators in the Fate of T Helper Cells. *Cell Commun Signal* (2017) 15:23–y. doi: 10.1186/s12964-017-0177-y
80. Hatakeyama S. Ubiquitin-Mediated Regulation of JAK-STAT Signaling in Embryonic Stem Cells. *JAKSTAT* (2012) 1:168–75. doi: 10.4161/jkst.21560
81. Trempe J. Reading the Ubiquitin Postal Code. *Curr Opin Struct Biol* (2011) 21:792–801. doi: 10.1016/j.sbi.2011.09.009
82. Turpeinen H, Ortutay Z, Pesu M. Genetics of the First Seven Proprotein Convertase Enzymes in Health and Disease. *Curr Genomics* (2013) 14:453–67. doi: 10.2174/1389202911314050010
83. Aittomäki S, Valanne S, Lehtinen T, Matikainen S, Nyman TA, Rämetsä M, et al. Proprotein Convertase Furin1 Expression in the *Drosophila* Fat Body Is Essential for a Normal Antimicrobial Peptide Response and Bacterial Host Defense. *FASEB J* (2017) 31:4770–82. doi: 10.1096/fj.201700296R
84. Radtke F, Wilson A, MacDonald HR. Notch Signaling in Hematopoiesis and Lymphopoiesis: Lessons From *Drosophila*. *BioEssays* (2005) 27:1117–28. doi: 10.1002/bies.20315
85. Sachan N, Mishra AK, Mutsuddi M, Mukherjee A. The *Drosophila* Importin- α 3 Is Required for Nuclear Import of Notch *In Vivo* and It Displays Synergistic Effects With Notch Receptor on Cell Proliferation. *PLoS One* (2013) 8:e68247. doi: 10.1371/journal.pone.0068247
86. Dansereau DA, Lunke MD, Finkielstein A, Russell MA, Brook WJ. Hephaestus Encodes a Polypyrimidine Tract Binding Protein That Regulates Notch Signalling During Wing Development in *Drosophila Melanogaster*. *Development* (2002) 129:5553–66. doi: 10.1242/dev.00153
87. Baillat D, Hakimi M, Näär AM, Shilatifard A, Cooch N, Shiekhattar R. Integrator, a Multiprotein Mediator of Small Nuclear RNA Processing, Associates With the C-Terminal Repeat of RNA Polymerase II. *Cell* (2005) 123:265–76. doi: 10.1016/j.cell.2005.08.019
88. Chen J, Wagner EJ. SnRNA 3' End Formation: The Dawn of the Integrator Complex. *Biochem Soc Trans* (2010) 38:1082–7. doi: 10.1042/BST0381082
89. Ghiglione C, Devergne O, Cerezo D, Noselli S. *Drosophila* Rala Is Essential for the Maintenance of Jak/Stat Signalling in Ovarian Follicles. *EMBO Rep* (2008) 9:676–82. doi: 10.1038/embor.2008.79
90. Kuraishi T, Nakagawa Y, Nagaosa K, Hashimoto Y, Ishimoto T, Moki T, et al. Pretaporter, a *Drosophila* Protein Serving as a Ligand for Draper in the Phagocytosis of Apoptotic Cells. *EMBO J* (2009) 28:3868–78. doi: 10.1038/embor.2009.343
91. Hashimoto Y, Tabuchi Y, Sakurai K, Kutsuna M, Kurokawa K, Awasaki T, et al. Identification of Lipoteichoic Acid as a Ligand for Draper in the Phagocytosis of Staphylococcus Aureus by *Drosophila* Hemocytes. *J Immunol* (2009) 183:7451–60. doi: 10.4049/jimmunol.0901032
92. Murray PJ. The JAK-STAT Signaling Pathway: Input and Output Integration. *J Immunol* (2007) 178:2623–9. doi: 10.4049/jimmunol.178.5.2623
93. Wang H, Chen X, He T, Zhou Y, Luo H. Evidence for Tissue-Specific Jak/STAT Target Genes in *Drosophila* Optic Lobe Development. *Genetics* (2013) 195:1291–306. doi: 10.1534/genetics.113.155945

Conflict of Interest: The authors declare that the research was conducted in the absence of any commercial or financial relationships that could be construed as a potential conflict of interest.

Publisher's Note: All claims expressed in this article are solely those of the authors and do not necessarily represent those of their affiliated organizations, or those of the publisher, the editors and the reviewers. Any product that may be evaluated in

this article, or claim that may be made by its manufacturer, is not guaranteed or endorsed by the publisher.

Copyright © 2021 Järvelä-Stölting, Vesala, Maasdorp, Ciantar, Rämets and Valanne. This is an open-access article distributed under the terms of the Creative Commons

Attribution License (CC BY). The use, distribution or reproduction in other forums is permitted, provided the original author(s) and the copyright owner(s) are credited and that the original publication in this journal is cited, in accordance with accepted academic practice. No use, distribution or reproduction is permitted which does not comply with these terms.